

## CHAPTER-4

### MATERIALS AND METHODS

#### 4.1 Materials

All chemicals and materials used in the study and the manufacturer's name are listed in Table 4.1. Instruments used in the study along with their manufacturer and model number are tabulated in Table 4.2 and the software used in the study is listed in Table 4.3.

**Table 4.1: List of chemicals/Materials used during the study.**

Chemicals/Materials	Source
Acetone	LOBA Chemie, India
Acetonitrile (HPLC grade)	S.D. Fine Chemicals Ltd., Mumbai, India
Arteether	Brooks Lab Ltd. Baddi, India (gift sample)
Buffer capsules pH $4.0 \pm 0.05$	Merck Specialities Pvt. Ltd., Mumbai, India
Buffer capsules pH $7.0 \pm 0.05$	Merck Specialities Pvt. Ltd., Mumbai, India
Dialysis membrane (MWCO-12 kDa)	Himedia Labs, Mumbai, India
Dichloromethane	Loba Chemie, Mumbai, India
Disodium hydrogen phosphate	Himedia Labs, Mumbai, India
Ethanol, absolute	Hong Yang Chemical Corporation, China
Eudragid 1100	S.D. Fine-Chem. Ltd., Mumbai, India
Glyceryl mono stearate	S.D. Fine-Chem Ltd., Mumbai, India
Hydrochloric acid	RANKEM, India
Iso-propyl alcohol	CDH, India
Lactose monohydrate	CDH, India
Magnesium stearate	CDH, India
Methanol (HPLC grade)	Loba Chemie, Mumbai, India
Microcrystalline cellulose (MCC)	CDH, India
Polyvinyl pyrrolidone (K30)	CDH, India
Potassium dihydrogen phosphate	CDH, India
Propylene Glycol	Loba Chemie, Mumbai, India
Sodium dihydrogen phosphate	Loba Chemie, Mumbai, India
Sodium hydroxide	CDH, India
Sodium starch glycolate	CDH, India
Stearic acid	S.D. Fine-Chem. Ltd., Mumbai, India
Talcum powder	CDH, India
Tween 20	Thermo Fisher Scientific India Pvt. Ltd, Mumbai, India
Tween 60	Thermo Fisher Scientific India Pvt. Ltd, Mumbai, India
Tween 80	Thermo Fisher Scientific India Pvt. Ltd, Mumbai, India
$\beta$ – Cyclodextrin	CDH, India

**Table 4.2: Equipment used during the experimental studies**

Equipment	Model Number	Manufacturer
Bath sonicator	Branson Ultrasonic cleaner 3210E-DTH TOSHCON-400KUS20	Branson Ultrasonics Corporation, Connecticut, USA Toshniwal Processing Instruments Ltd., New Delhi,
Centrifuge	Bench Model Remi R-24 Remi C-24	Sartorius, Germany Remi Motors, Mumbai, India
Cold centrifuge	Biofuge Primo R Heraeus	Thermo Scientific, Vienna, Austria
Deep freezer (-20°C)	Vertical Deep Freezer FS- 345 (345 L)	Blue Star, Mumbai, India
Deep freezer (-80°C)	V-410 Ultra low freezer	New Brunswick Scientific, France
Differential scanning calorimeter	DSC 821e DSC-Q20	Mettler Toledo, Switzerland TA Instruments, USA
Dissolution apparatus	DS8000	Lab India Pvt. Ltd., Navi Mumbai
Franz diffusion cell assembly	Stirrer: V6B Franz cells: 4G-01-00-20-30	PermGear Inc., USA
Freeze dryer	SNL216V-230  Alpha 2-4 LD Plus	Thermo Electron (Thermo Sawant), USA Martin Christ GmbH, Germany Vir Tis, Wizard 2.0, New York, U.S.A
FTIR	RX-100	Perkin Elmer, U.S.A.
High-performance liquid chromatography (HPLC)	Waters® 2695 Separation Module equipped with 2996 Photodiode Array Detector	Waters, Milford, USA
Hot air oven	NSW	Narang Scientific, New Delhi, India
Hot air oven	SILHAOG-04	Gupta Scientific Industries, Ambala
Hot plate	1609123	Gupta Scientific Industries, Ambala
HPLC Column	Hibar® 250mm x 4.6 mm HPLC column Purospher STAR RP-18 end-capped, 5 µm particle size	Merck KGaA, Germany
Magnetic stirrer	2020/51/DG	Amar Enterprises, Ambala
Magnetic stirrer (Thermostatic)	1MLH, 2MLH Spinot™	Remi Motors, Mumbai, India Tarsons Products, Calcutta, India
Mechanical stirrer	RQ 122	Remi Motors, Mumbai, India
Melting point apparatus	S-973	Amar Enterprises, Ambala
Membrane filtration assembly	25 mm, 47 mm	Millipore, USA
Micropipettes	LABQUEST-01521853	Thomas Scientific, USA
Microscope (optical)	TELAVAL 31 Nikon eclipse 80i	Carl Zeiss, Germany Nikon Corporation, Japan
Microscope, attached with a camera and fluorescence filters	TE 2000-S, camera DS-5M- L1	Nikon Corporation, Japan
Particle size analyzer	Beckman Coulter, Delsa Nano Particle Analyzer	Malvern Instruments Limited, UK
pH meter	L1-120 Cyber Scan 510	ELICO, Mumbai, India Eutech Instruments Pvt. Ltd., Singapore

pH meter	Phan Pico+	Labindia, Mumbai, India
pH meter	RG-101-02	Amar Enterprises, Ambala
Pipettes	71050XET, 720020 and 720070	BIOHIT OYJ, Finland
Purified water system	IQ7003/05/10/15	Millipore, India
Refrigerator	GL-478/2008; 422 L	LG, India
Rheometer	Rheolab QC HS 143 – Rheometer	Anton Paar Rheometer, Germany
Rotary evaporator	RE121	Buchi, Switzerland
Scanning electron microscope	JSM-6100	Japan Electron Optics, Japan
Shaking water bath	NSW 133	National Scientific Works, Delhi, India
Shaking water bath	NSW 133	Narang Scientific Works, New Delhi, India
Transmission electron microscope	H-7000, fitted with a Mega View II digital camera	Hitachi Ltd., Japan
Triple distillation assembly (Glass)	H-456	Scientronic, Germany
UV-visible spectrophotometer	Genesys 6 Spectro-UV-Vis-Dual beam, 8 Autocell, UVS-2700	Shimadzu Corporation, Japan
Vacuum pump	Welch Automatic Vacuum pump	Welch Rietschle Thomas Skokie, USA
Vortex mixer	CM101	Remi Motors, Mumbai, India
Vortex shaker	LABVS90	Amar Enterprises, Ambala
Water bath	0828	Amar Enterprises, Ambala
Weighing balance (electronic)	AE240, BB244	Mettler Analytical Balances, Switzerland

**Table 4.3: List of softwares used during the study.**

Software	Purpose
Biorender	To draw figures
Design Expert 13	Quality by design approach for formulation development
EMPOWER-2	HPLC
Microsoft Office, 2010	Documentation
Minitab	Statistical analysis
Nicolet Omnic	IR Analysis,
UV Lambda 25	UV Spectroscopy, standard analysis
TriplotV14 software	Todd A. Thomson, Informer Technologies, California, USA

## **4.2 Calibration of glassware and instruments**

### **4.2.1 Calibration of thermometer**

The melting point was then determined using the capillary tube method. The melting point of benzoic acid was used to calibrate the thermometer. A small amount of benzoic acid was collected and placed in the capillary tube for this purpose (IP, 2019).

### **4.2.2 Calibration of measuring cylinder**

The empty measuring cylinders (10 mL and 100 mL) were weighed. Water was carefully poured into measuring cylinders, which were then carefully emptied into the beaker (IP, 2019). The container with water was reweighed and the volume of the measuring cylinder was calculated by using following formula:

$$\frac{\text{Volume of water delivered}}{\text{Observed volume}} = \frac{\text{Volume of water in measuring cylinder}}{\text{Density of water}} \dots\dots\dots (1)$$

### **4.2.3 Calibration of analytical balance**

Calibration of an analytical balance (Mettler Analytical Balances, Switzerland) was done by adjusting the internal and external weight as per the standard SOP No. TCM/03.

### **4.2.4 Calibration of pipettes**

A dry empty beaker was weighed. The pipette was loaded with water at a predetermined recorded temperature and used an appropriate pipette handling method to deliver the entire water into the beaker. Finally, the container was reweighed with water, and the volume of the pipette was calculated by using following formula:

$$\frac{\text{Volume of water delivered}}{\text{Observed volume}} = \frac{\text{Volume of water in measuring cylinder}}{\text{Density of water}} \dots\dots\dots (2)$$

### **4.2.5 Calibration of pH meter**

For calibration of the pH meter (Amar Enterprises, Ambala), reference buffer solutions of pH 4.01 and 6.87 were prepared and calibration was done as per SOP No. TCM/01.

### **4.2.6 Calibration of UV spectrophotometer**

The UV Spectrophotometer (Shimadzu Corp, Japan) was calibrated using the standard process outlined in IP 2019. The stray light limit, resolving power, and absorbance control were all assessed and compared to industry standards (IP, 2019).

### 4.3 Preformulation studies

The physical and chemical properties of the active drug moiety are determined in the preformulation study to design a safe, effective, and stable dosage form. The nature of the active drug moiety has a direct impact on formulation development factors such as entrapment efficiency, compatibility, solubility, dissolution rate, and pharmacokinetic response. The preliminary objective of the preformulation phase or study is to lay down the foundation for transforming a new drug entity into a pharmaceutical formulation in such a way that it can be administered in the right way, in the right amount, and on perhaps the most important at right target (Honmane, 2017). The development of beneficial pharmaceutical dosage forms requires various preformulation parameters as described in Fig. 4.1.

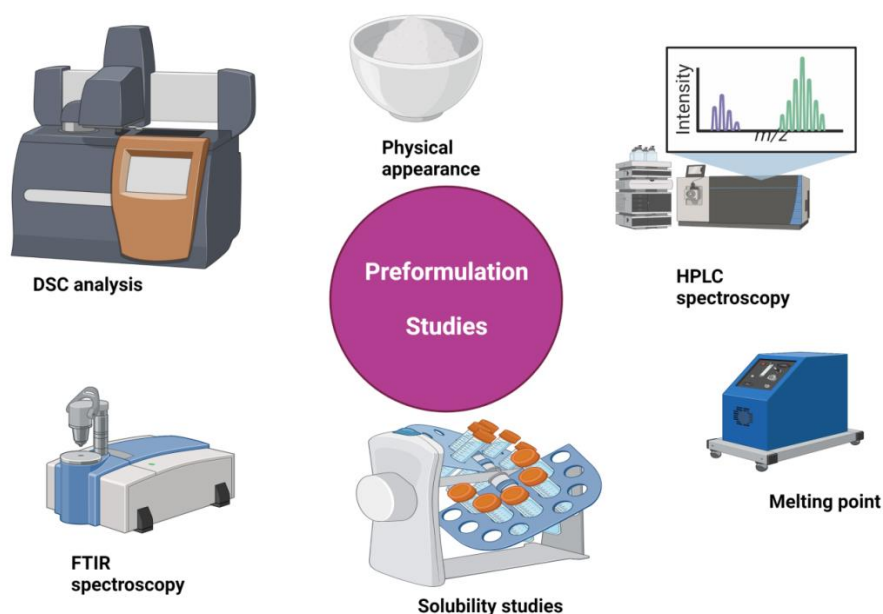


**Figure 4.1: Parameters for preformulation studies.**

#### 4.3.1 Drug identification

Pure drug (ART), was obtained from Brooks Lab. Ltd. India as a gift sample. Obtained drug sample was identified according to the standard specifications given below.

#### 4.3.2 Physical appearance

The physical appearance of the obtained drug was reported by visual observation.

#### **4.3.3 Melting point**

The melting point of a substance is a criterion for its purity and identification. The melting point of ART was determined using a capillary melting point instrument. The thermometer was calibrated before the melting point was determined. The melting point of a little amount of ART was measured in the capillary tube.

#### **4.3.4 Solubility studies**

The pharmacopeial approach was used to determine solubility. One part of ART was added to various solvents such as methanol, dichloromethane, oleic acid, and water, and the solutions were shaken reciprocally for 5 min at 37 °C. The drug's solubility was evaluated and compared to reference data.

#### **4.3.5 FT-IR Spectroscopy**

FT-IR spectra were recorded for identification and to check the purity of procured drug ART, and hydrophilic polymers (PEG-6000, Poloxamer-407, Soluplus). The IR spectrum of pure drug and hydrophilic carriers was conducted by using FTIR-8400S (Shimadzu, Japan). In dry KBr, a total of 2% (w/w) of the sample was combined. The sample was mixed with a mortar/pestle before being compressed onto a KBr disc at 10,000 psi in a hydraulic press. Over a wave number range of 500–4000  $\text{cm}^{-1}$ , each KBr disc was scanned 32 times at 4 mm/sec at a resolution of 2  $\text{cm}^{-1}$ . The characteristic bands were recorded and compared against reported values (Ansari *et al.*, 2011).

#### **4.3.6 DSC analysis**

DSC analysis of the pure drug ART, and hydrophilic carriers (Soluplus, PEG 6000, and Poloxamer 407) was carried out using Perkin Elmer 4000, (USA). Under purged nitrogen gas at a flow rate of 50 mL/min, samples were heated at a rate of 5 °C/min over a temperature range of 50 °C to 350 °C. Prior to the observations, the equipment was calibrated for temperature and heat flow at 5 °C/min using Nickle as reference material. All measurements were done with 5-10 mg of sample material in sealed non-hermetic aluminium pans (Lang, 2013).

#### **4.3.7 XRD analysis**

The XRD patterns of pure drug ART and hydrophilic carriers (Soluplus, PEG 6000, and Poloxamer 407) were examined through PANalytical Xpert Pro (Netherlands).

Operating parameters for X-ray diffraction studies include the targeting of CuK $\alpha$ , with a current of 30-mA and input voltage of 40KV. A system of receiving, diverging, and anti-scattering slits of 1°, 1°, 1°, and 0.15°, respectively was used. The patterns were obtained between the 2 $\theta$  range in the diffraction angles range of 5-50 by employing the scanning step size of 0.04° (Utami *et al.*, 2021).

#### 4.3.8 Quantitative analysis using UV spectroscopy

##### 4.3.8.1 Standard stock solution preparation

ART (10 mg) was weighed accurately and dissolved in ethanolic phosphate buffer solution pH 6.8 to prepare the stock solution of concentration equals to 1000  $\mu$ g/mL concentration. Exactly measured volumes ( 0.4 mL to 1.8 mL) was taken from the stock solution in 10 mL volumetric flasks and around 2.0 mL of 5M HCl solution was added to each. The solutions were maintained in a water bath at 50 $\pm$ 2°C for 30 minutes for acid degradation. Finally, ethanolic PBS 6.8 was used to make a volume of up to 10 mL. Using ethanolic PBS 6.8 and HCl (8:2) as a blank, the absorbance was measured at 254 nm wavelength. A calibration curve was produced by constructing a graph between absorbance and corresponding concentrations at this wavelength maximum.

The analytical method development for ART was validated as per ICH Q8 (R2) guidelines along with implementing the QbD approach as discussed in Fig 4.2.

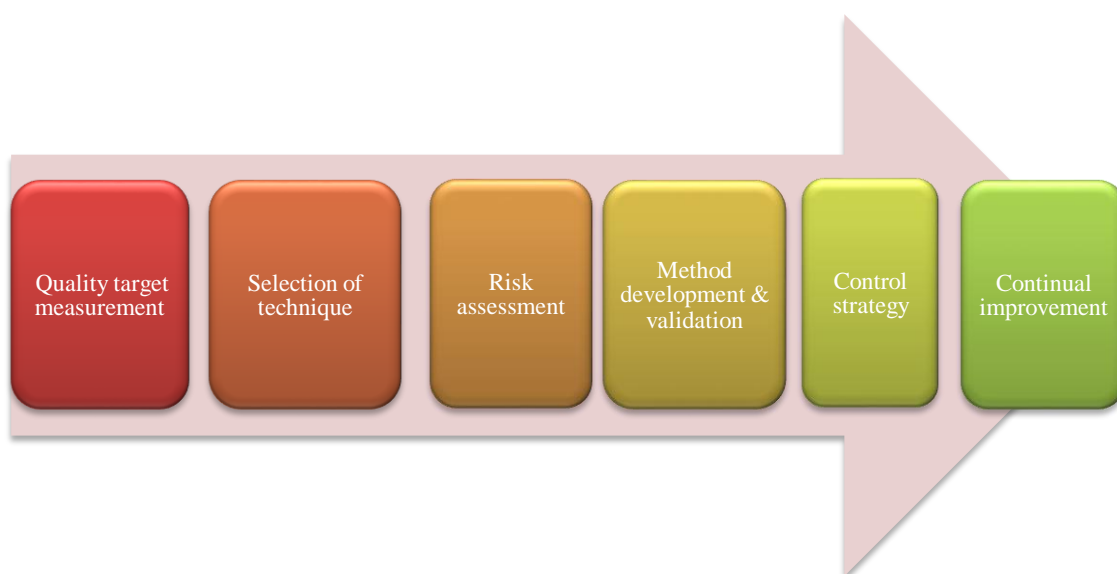


**Figure 4.2: Quality by design approach to analytical method development.**

#### **4.3.8.2 Design of method**

The most important step in any research project is to design the method, which entails first researching and understanding the quality method development requirements, and then carrying out the experiment while keeping in mind the critical method variables that must be controlled for the method to be rugged and robust.

The next step is to determine if the experiment's goal satisfies the conditions for understanding the Analytical Target Profile (ATP) for the technique. Hence, the spectrophotometric technique is used to determine the amount of ATP in any molecule.

#### **4.3.8.3 Development of method**

Once the ATP has been established, the researcher must choose the best approach and circumstances to satisfy the ATP's criteria.

#### **4.3.8.4 Risk assessment**

Understanding the influence of major input factors on the technique's performance characteristics is critical for developing a robust and tough analytical approach. In method development, risk assessment is done using a fishbone diagram and a Failure Modes and Effects Analysis (FMEA) which are used to specify which factors can be managed to reduce risk. Risk identification and risk analysis are the most important parts of risk assessment methodology, according to ICH Q9 standards. The risk was identified using an Ishikawa fishbone diagram, which depicted all conceivable aspects that may affect the technique development. The Critical Analyte Attribute (CAA) and variables involved in method development were identified as the first phase. Following the study of the Ishikawa fishbone diagram, several technique factors such as sample/instrument scanning speed, solvent kinds, sampling interval, sample integrity, and so on were investigated.

Important key parameters were also exposed to suitable optimization design to establish the best amount of variables for obtaining the predefined analytical goal profile.

#### **4.3.8.5 Experiment design (ED)**

After deciding on the variables, such as the quantity of HCl to be used for acid degradation of ART and the pH of the ethanolic phosphate buffer, a design of the



experiment was created to guarantee that the most information was gathered while limiting the number of tests. Different measurements of attributes such as accuracy or precision may be assessed depending on the kind of technique. Design Expert software version 13.0.5.0 was used to determine the relationship between the independent and dependent variables. All of the experiments in the optimization studies were carried out in triplicate. The QbD-based treatment of an analytical method's robustness necessitates the evaluation of all characteristics (factors) that most significantly impact selectivity (results), both alone and in combination. Various approaches may be used to calculate effects and interactions, equation coefficients, and statistical significance of coefficients that have been obtained. ANOVA based on the Student's t-test may be used to calculate the significance of coefficients (Tome et al., 2019). A simple mixture design was used to determine the stock solution and subsequent dilutions to be prepared, yielding 13 experimental runs for three components.

By entering the data into the Design Expert software, the relation between dependent and independent variables was predicted and a suitable mathematical model in the form of a polynomial equation (Equation 1) was developed.

$$Y = 0 + 1A + 2B + 3AB + 4A^2 + 5B^2 \dots\dots\dots (1)$$

Where Y denotes the measured response, 0 denotes the intercept, 1 and 2 denote the first-order parameters of the two chosen variables A and B, 3 denotes the coefficients of an A and B correlation term, and 4 and 5 denote the coefficients of quadratic of selected factors, and 4 and 5 denote the coefficients of quadratic of selected factors. Equation 1 is a linear second-order model that arises from the quadratic terms. The positive and negative signs of each coefficient were used to select synergistic and antagonistic effects from the polynomial equations.

#### **4.3.8.6 Method design output**

A set of method conditions were established and described that are expected to meet the ATP. ANOVA was used to properly examine the significance of each model using the Lack of Fit and Goodness of Fit statistics before selecting a model and f value, p-value, accuracy value, and  $R^2$  adjusted were determined. Different polynomial equations were created with significant p values less than 0.5. Also, with help of software the plots like Normal plots, Predicted vs Actual plots, Residual vs Predicted

plots, and Residual vs Run plot were created to analyze the behaviour or effect of the ratio of ethanol, phosphate buffer, and HCl used as independent variables on the dependent variables or responses (absorbance at 254 nm). Model graphs demonstrated how the response likely evolves at various amounts of variables at different times using a predicted response equation with individual coefficients. With help of 3-D response surface plots, the behavior of the system was analysed by evaluating the contribution of the independent factors. The contour plots display slices of the response surface. A normalized plot is a graphical representation of a response plotted between normalized factor levels (N) and a response variable (Awotwe-Otoo *et al.*, 2012). These are only shown when the component levels are not equidistant, i.e. when the middle level is not the mean of the high and low levels. 2D contour plots and 3D response surface plots were used to demonstrate the relationship between the selected independent method variables and response variables. Following the development of the design space, a minimum of three confirmatory experimental runs were undertaken within the design space's designated range for verification.

#### **4.3.8.7 Validation of ED**

The point prediction feature was applied to acquire the value of the answers at specific values of method variables in design space for further optimisation of the method for analyzing the applicability or functioning of the generated model in a lab scale. The optimal value of replies was compared to the values of responses obtained by experimenting on a lab scale with identical procedure variables. This comparison confirmed the proposed polynomial model-based predictions in an analytical lab under real-world conditions.

#### **4.3.8.8 Conditions for spectrophotometry**

A standard solution of ART was scanned in the spectrum range from 400 nm to 200 nm to determine the analytical wavelength. The maximum wavelength of ART after acid degradation, 254 nm, was chosen for method development from the spectrum.

#### **4.3.8.9 Method validation**

Validation is one of the most critical aspects of developing a reliable, robust, and repeatable UV spectrophotometric analytical technique that will be accepted by the industry. It's critical to determine how robust or tough a new approach is when it's optimized. According to the ICH Q2(R1) guideline, the improved UV

spectrophotometric technique was verified for specificity, accuracy, repeatability, linearity, precision, intermediate precision, robustness, and system appropriateness.

Precision, Linearity, robustness, accuracy, limit of detection (LOD), and limit of quantification (LOQ) were used to validate UV method.

#### **4.3.8.9.1 Linearity analysis**

0.4 to 1.8 mL of stock standard solution were added to 10 mL of a volumetric flask, along with 2 mL of 5M HCl. The HCl solution was added to each concentration, at  $50\pm 2^{\circ}\text{C}$  for 30 min to allow the acid to decompose, yielding,  $\alpha$ ,  $\beta$ - unsaturated decalone (8-methyl-5-(2-propenyl) decalin-4-ene3-one). Finally, each solvent was used to make a volume of up to 10 mL, resulting in a drug concentration of 2 to 20  $\mu\text{g/mL}$ . Using ethanolic PBS 6.8 and HCl (8:2) as a blank, the absorbance was measured at 254 nm wavelength. The calibration curve was plotted as drug concentration vs absorbance at this wavelength maximum. The y-intercept, slope, and correlation coefficient of the regression equation were presented.

#### **4.3.8.9.2 Precision**

The accuracy (intra-day and inter-day) of the developed method was determined using percent relative standard deviation (percent RSD). The study utilized approx. three times a day for intra-day accuracy and inter-day precision (separate day). The % RSD was calculated using values of concentration for intra-day and inter-day precision six times each.

#### **4.3.8.9.3 Accuracy**

Excipients utilized in the dosage form were evaluated for interference with the suggested approach, and recovery tests were done using the conventional addition method. The quantity of standard recovered was calculated as a mean recovery with percent relative standard deviation upper and lower limits. To evaluate the accuracy of the analytical approach, three dilutions of market formulation with the same concentration were spiked with various concentrations of standard drug solution, i.e. 80%, 100%, and 120%.

#### **4.3.8.9.4 Robustness and ruggedness**

The capacity of an analytical approach to survive small but deliberate changes in method parameters is measured by its robustness. Analyses at different wavelengths and deliberate small changes in the concentration of solvent used were used to prove

the resilience of the proposed method. The absorbance was measured, and the percentage of RSD was calculated. The method's robustness may be described by the Relative robustness value generated in an intra-laboratory experiment, while the method's ruggedness is defined by the Relative ruggedness value established in inter-laboratory studies. The higher the relative robustness or relative roughness score, the more robust or rough the approach will be.

#### **4.3.8.9.5 Detection and quantification limits (UV spectroscopy)**

The detection, as well as quantification limits, were calculated using a method based on the calibration plot's standard deviation (s) and slope (S).

$$\text{LOD} = 3.3s/S \text{ and } \text{LOQ} = 10s/S \dots\dots\dots (2)$$

### **4.3.9 Quantitative analysis using HPLC**

#### **4.3.9.1 HPLC method design**

The method designing stage entails determining method performance criteria, developing a method that fits these requirements, and then doing the appropriate research to identify the critical method variables that must be handled to guarantee the technique is rugged and robust.

#### **4.3.9.2 HPLC method performance ratios**

The objective requirements for the method's intended usage should be described using the QbD technique, which stands for method Analytical Target Profile (ATP). As a result, chromatographic methods may be used to estimate the ART's ATP. To fulfill the ATP criteria, an acceptable method condition and procedures must be specified once the ATP has been created (Bansal *et al.*, 2016)

#### **4.3.9.3 Understanding HPLC method**

The robustness and ruggedness concerns based on risk assessment and estimate the influence of variables on method performance characteristics, allowing us to analyze operational method controls (Trueman *et al.*, 2016).

#### **4.3.9.4 HPLC method risk assessment.**

Experiments are carried out to find the most efficient link between technique performance and input factors. The information gathered during the development and

execution of the approach was entered into a risk assessment (using an FMEA or Fishbone diagram) that is used to determine the factors (Dejaegher *et al.*, 2011).

#### **4.3.9.5 HPLC method experimental design**

The DoE methodology was used to optimize the method and to understand the analytical process in a better way with lesser number of experiments.

##### **4.3.9.5.1 HPLC method design output**

The QbD methodology was used to assess all elements that impact the findings individually or in combination for the robustness of the HPLC based analytical procedure. Statistical investigations, such as Central Composite Design was utilized for this, and automated robustness trials to lessen the experimental burden and varied problems. Retention time and resolution were selected as critical criteria that might influence the final quality metrics (Hibbert, 2012).

As a result, the Design-Expert software version 13.0.5.0 was used to optimize the three elements simultaneously (State-Ease Inc, USA). Flow rate, percent of mobile phase, and pH were chosen as independent variables, whereas retention time and resolution were selected as responses or dependent variables. Table 4.4 shows the results of a response surface study type and central composite design in which three components produced 20 runs. The experiment method was used in this study not only to determine the optimal value of the chosen crucial variables but also to show the correlation between the independent and dependent variables.

**Table 4.4: Runs created for optimization of critical factors.**

Std	Run	A: pH of mobile phase	B: Flow rate (mL/min)	C: ACN in water (%)
14	1	5	0.55	76.8179
13	2	5	0.55	43.1821
15	3	5	0.55	60
19	4	5	0.55	60
20	5	5	0.55	60
4	6	7	1	50
6	7	7	0.1	70
9	8	1.63641	0.55	60
8	9	7	1	70
16	10	5	0.55	60
7	11	3	1	70
11	12	5	0.206807	60
5	13	3	0.1	70
2	14	7	0.1	50
10	15	8.36359	0.55	60
12	16	5	1.30681	60
1	17	3	0.1	50
17	18	5	0.55	60
18	19	5	0.55	60
3	20	3	1	50

#### 4.3.9.5.2 Chromatographic conditions

The chromatographic column utilized was the Sunfire C-18 (250 mm x 4.6 mm, 5  $\mu$ m). The chemicals were separated using a gradient program of acetonitrile and water mobile phase with a 20  $\mu$ L/min injection volume and a flow rate of 0.5 mL/min. The ratio of acetonitrile and water used was 60:40 (v/v). The column temperature was maintained at 30°C, and the detection was done at a wavelength of 214 nm (Musters *et al.*, 2013). The parameters used for method development are given in Table 4.5.

**Table 4.5: Parameters for HPLC-based quantitative analysis of ART.**

Mobile phase	Acetonitrile: Water (60:40)
Column	SunFire C <sub>18</sub> column 250 nm X 4.6 mm (5 µm)
Column temperature	30 °C
Quantification wavelength	214 nm
Injection volume	20 µL/min
Run time	10 min
Detector	Waters 2489 UV/Visible detector
Make/ Model	Waters, USA/ Waters 1525
Software	Empower software (EMPOWER-2)
Retention time (R <sub>t</sub> )	5.6 min

#### **4.3.9.5.3 Validation of the proposed HPLC method**

It was verified after chromatographic technique development and optimization. The validation of analytical method verifies the method's features meet the application domain's criteria. Using ICH recommendations, as per Q<sub>2</sub> R<sub>1</sub> guidelines the suggested approach was verified for linearity, precision, accuracy sensitivity, and recovery (Ojha *et al.*, 2022).

##### **4.3.9.5.3.1 Linearity (HPLC method)**

Six different concentrations of ART were tested in triplicate to evaluate linearity, and a calibration curve was constructed in the necessary range of 5-20 ng/mL. A calibration curve was generated using replicate analysis at all concentration levels, and the linear connection was analysed using the least square approach in the Microsoft Excel application.

##### **4.3.9.5.3.2 Precision (HPLC method)**

The developed method's intra-day accuracy and inter-day precision were assessed in R.S.D. For intra-day precision, the trials were performed three times a day, and for inter-day precision, experiments were repeated three times on three different days. The % relative standard deviation was computed six times for both intraday and interday precision concentration values. Finally, the mean percent R.S.D. (percent R.S.D. = (S/X) 100, where S is the standard deviation and X is the mean of the sample under investigation) was used to conclude (D'Avolio *et al.*, 2010).

##### **4.3.9.5.3.3 Accuracy (HPLC method)**

Recovery tests were carried out using the usual addition technique to test the accuracy of the proposed approach and to check for interference from excipients included in the dose form. The trial was carried out by adding known quantities of the commercial formulations i.e.  $\alpha,\beta$ -ART (*i.m.* injection). The amounts of standard recovered were computed in terms of mean recovery with % relative standard deviation upper and lower bounds. Three identical dilutions of market formulation were spiked with varying concentrations of the common solution, i.e., 80%, 100%, and 120%, to determine the accuracy of the analytical technique. The area of these solutions was measured and then plotted onto a calibration curve. The concentrations and accuracy of the samples were calculated.

#### **4.3.9.5.3.4 Robustness (HPLC method)**

An analytical procedure's robustness measures its ability to stay unaffected by small but purposeful variations in technique parameters. The suggested method's robustness was established by analyzing it at multiple wavelengths (around 214) and making minor modifications in the solvent concentration (6:4) employed. The absorbance of each sample was recorded, and the result was expressed as RSD (%).

#### **4.3.9.5.3.5 Detection and quantification limits (HPLC method)**

The detection and quantification limits were computed using following equations based on the standard deviation (s) and slope (S) of the calibration plot.

$$\text{LOD} = 3.3s/S, \dots\dots\dots (3) \text{ and}$$

$$\text{LOQ} = 10s/S, \dots\dots\dots (4)$$

#### **4.3.9.5.3.6 Percentage purity (HPLC method)**

Ten mg of powder was carefully weighed and diluted sufficiently with acetonitrile to acquire a concentration that falls within the concentration range. After that, the samples were tested in triplicate (Zou & Koh, 2007).

### **4.4 Solubility enhancement techniques**

#### **4.4.1 Hydrotropic solubilization of ART**

In distilled water, 40% w/v solutions of each hydrotropic agent, namely sodium benzoate (SB), urea, nicotinamide (NIC), and sodium citrate (SC), were prepared (Ansari *et al.*, 2010). Solubility was determined by mixing 5 mg of ART with 2 mL of the hydrotropic mixture in a 10 mL volumetric flask and agitating for 15 min on a



vortex shaker. After a 15 min break, 0.5 mL of the hydrotropic blend was added to the mixture again. The drug was entirely dissolved in the hydrotropic mix after each addition of 0.5 mL to the solution. Approximately 10 mL of the hydrotropic blend was added to the drug solution. Following that, the quantity of hydrotropic mix necessary to dissolve 5 mg of drug was recorded, and the increase in solubility was computed using the drug's solubility in distilled water as a reference.

#### 4.4.1.1 Mixed hydrotropic solubilization

To make a transparent solution, two hydrotropic agents were combined as stated in Table 4.6, and dissolved in water. Solubility was determined by mixing 5 mg of ART with 2 mL of the hydrotropic mixture in a 10 mL volumetric flask and agitating for 15 min on a vortex shaker. After a 15 min break, 0.5 mL of the hydrotropic blend was added to the mixture (Ansari *et al.*, 2010). The medication was entirely dissolved in the hydrotropic mix after each addition of 0.5 mL to the solution. Up to 10 mL of the hydrotropic blend was added to the medication combination. Following that, the quantity of hydrotropic mix necessary to dissolve 5 mg of medication was recorded, and the increase in solubility was computed using the drug's solubility in distilled water as a reference.

**Table 4.6: Mixed hydrotropic blend compositions.**

S. No.	Hydrotropic agents	Concentration (%)
1.	Nicotinamide + Sodium benzoate	20+20
2.	Nicotinamide + Sodium benzoate	10+30
3.	Nicotinamide + Sodium benzoate	30+10

After solubility improvement, the ART and hydrotropic blend combination was transferred to a petri dish and set on a hot plate. Water was evaporated by continuous stirring, and the solid mass of the drug and the hydrotropic mix was collected and kept at  $27 \pm 2$  ° C.

#### 4.4.2 Solid dispersion

The solid dispersion was prepared using two different processes as explained below:

##### 4.4.2.1 Solvent evaporation method

The solvent evaporation approach involves solubilizing the drug and carrier in a volatile solvent and then evaporating it.

The drug ART and carriers were equally dissolved in enough ethanol to evenly dissolve the drug ART and carriers in a china dish in the weight ratios given in Table 4.7. Any leftover ethanol in the mixture was then evaporated in a hot air oven at  $50 \pm 2$  °C. The mixture was collected and stored at  $27 \pm 2$  °C in amber-colored glass containers.

#### 4.4.2.2 Melting procedure

During the melting process, the carrier is heated slightly over its melting point, and the active drug is suspended in the matrix (Ansari *et al.*, 2015).

To develop melt combinations, the drug ART and carriers were mixed in the ratios listed in Table 4.7. In a pestle and mortar, samples were crushed for 5 min. This physical mixture was heated to melting point temperature in a water bath, then swirled constantly until entirely melted. An ice bath was used to solidify the melting liquid. After that, the mixture was collected and put into amber-colored glass containers that were maintained at 37 °C.

**Table 4.7: Composition of various solid dispersions of ART.**

Composition	Method	Ratio (w/w)
ART:PEG-6000	Melting	1:1, 1:2, 1:3, 1:4, 1:5
ART:Poloxamer-188	Melting	1:0.5, 1:1.5, 1:2.5, 1:3.5, 1:4.5
ART:Poloxamer-407	Melting	1:0.5, 1:1.5, 1:2.5, 1:3.5, 1:4.5
ART:PVP K-30	Solvent evaporation	1:0.25, 1:0.5, 1:1, 1:2, 1:3, 1:4
ART:HPMC E 15LV	Solvent evaporation	1:1, 1:2, 1:3, 1:4, 1:5
ART:HPMC K 100M	Solvent evaporation	1:1, 1:2, 1:3, 1:4, 1:5
ART:Sucrose	Solvent evaporation	1:1, 1:2, 1:3, 1:4, 1:5
ART:Mannitol	Solvent evaporation	1:1, 1:2, 1:3, 1:4, 1:5
ART:D-Fructose	Solvent evaporation	1:1, 1:2, 1:3, 1:4, 1:5
ART:Dextrose	Solvent evaporation	1:1, 1:2, 1:3, 1:4, 1:5
ART:Saccharin sodium	Solvent evaporation	1:1, 1:2, 1:3, 1:4, 1:5
ART:D-Tartaric acid	Solvent evaporation	1:1, 1:2, 1:3, 1:4, 1:5
ART:Starch soluble	Solvent evaporation	1:1, 1:2, 1:3, 1:4, 1:5
ART:Succinic acid	Solvent evaporation	1:1, 1:2, 1:3, 1:4, 1:5
ART: $\beta$ CD:PEG600:Pol - 407	Melting method	1:1:3.7:4.3

#### 4.4.2.3 Characterization of solid dispersions and hydrotropic solid dispersion

The solubility and dissolution patterns of prepared solid dispersions and hydrotropic solid dispersions of  $\alpha, \beta$ -ART were investigated. DSC, FT-IR spectroscopy, and XRD

analyses were used to evaluate the spectrum data, as well as particle size and zeta potential (Chutimaworapan *et al.*, 2000).

#### **4.4.2.4 Permeability study of prepared solid dispersion**

The permeability of the gut of a pig was evaluated in triplicate using the Franz diffusion cell procedure (Ansari *et al.*, 2014). In this work, Franz diffusion cells with a 13.3 mL receptor compartment and a 1.79 cm<sup>2</sup> diffusion area were employed. The receiver compartment of the diffusion cells was then carefully attached to a circular piece of intestinal skin. The skin operated as a seal between the two half-cells when the donor compartment was clamped to the receptor compartment. The receptor medium was phosphate buffer solution (pH 6.8), and air bubbles in the receiver compartment were avoided by flowing water through the bottom compartment's jacket and stirring regularly using a magnetic stirrer. The testing was conducted by removing 1 mL of the test and replacing it with the same volume of fresh media to ensure sink conditions at the predetermined time points of 15, 30, 60, 90, 120, 240 and 360 min. The collected sample was adequately diluted before being injected into an HPLC for drug analysis. After the permeation research was completed, the Franz diffusion cell was disassembled and the skin (from the diffusion study) was carefully removed from the cell. The phosphate buffer pH 6.8 was used to swab the formulation on the skin's surface (Gorajana *et al.*, 2015). To ensure that no residues of the formulation remained on the skin's surface, the process was performed again. To extract the medication contained in the skin, the skin was sliced into tiny pieces and maintained in a buffer pH of 6.8. The quantity of drug deposited in the skin was then determined by HPLC following appropriate dilution and filtering.

#### **4.4.3 Cyclodextrin complexation**

##### **4.4.3.1 Optimization of prepared cyclodextrin complexes**

A design of experiment technique was used to comprehensively examine the, ART- $\beta$ -cyclodextrin complex. Because the complex of ART with cyclodextrin was in ratios, a simple lattice mixture plot was used. Experiment design with two components, ART- $\beta$ -cyclodextrin, with % drug release and solubility enhancement as responses. Because the components are both categorical and continuous, a mixture design was adopted based on the Scheffé model.

The Design-Expert® 13 software was used to generate the level II optimum coordinate exchange design type (Stat-Ease Inc., Minneapolis, MN). The Level II ideal design was selected because it had a reduced average prediction variance over the experimental zone. The design model was reduced quadratic and main impacts after 8 runs.

The statistical analysis provided by Design Expert Software Version 13 was used to discover a stronger link between the independent and dependent variables. Responses in the polynomial model (cubic, linear, quadratic, or special cubic) were altered, and equations describing the relationship between the independent and dependent variables were shown as mathematical equations. Various statistical factors available in Analysis of Variance (ANOVA), such as p-Value,  $R^2$  value, and acceptable accuracy, were employed to determine a viable mathematical model. The constructed model was then utilized to identify the desired results using the Design Expert Software's desirability function and experimentally validated.

#### **4.4.3.2 Analysis of phase solubility of ART-CD complex**

The experiment of phase solubility was performed to compute the ratio of the ART-CD-complex in the solution phase. In brief, ART (10 mg) was suspended in a pH 6.8 phosphate buffer saline (PBS) solution containing 1-20 mM of CD. The samples were agitated on an orbital shaker at 200 rpm for 48 h at 37°C. After 48 h, the absorbance was measured using HPLC.

Eq. 5 was used to derive the apparent stability constant was computed from the slope of the phase-solubility diagram.

$$\text{Slope}/S_0 = K_c (1 - \text{Slope}) \dots\dots\dots (5)$$

Where  $S_0$  is the solubility of the drug without cyclodextrin and  $K_c$  is the apparent stability constant.

#### **4.4.3.3 Preparation binary and ternary complexes of ART - $\beta$ -CD**

To prepare solid inclusion complexes of ART with  $\beta$ -CD, physical mixing, kneading, and spray drying techniques were performed (molar ratio) as shown in Fig 4.3. Physical mixes were created by combining a certain amount of medicine with the  $\beta$ -CD of choice in a mortar to create a uniform mixture. The selected  $\beta$ -CD were triturated in a mortar with a little quantity of solvent (water:ethanol) in the kneading

technique (KN) (1:1). The drug was administered gradually. The viscous slurry was kneaded for 90 min before being vacuum dried for 24 h at  $30 \pm 2^\circ\text{C}$ . The dried material was crushed and sieved through a 150 micron filter. In spray drying the drug and selected  $\beta$ -CD were dissolved separately in a tiny quantity of ethanol (SD). Both solutions were mixed together, and the finished product was spray dried using a spray dryer. In the instance of  $\beta$ -CD, it was dissolved in hot water before being added to and well mixed with the drug solution. Spray drying was performed under the following conditions: 1 mL/min flow rate,  $80^\circ\text{C}$  input temperature,  $40$ - $50^\circ\text{C}$  exit temperature, and a vacuum of 110-120 mmwc. In the ternary complexes, the identical technique was followed, but only 0.20% PVP K 30 at equimolar amounts of, ART, and  $\beta$ -CD was added.

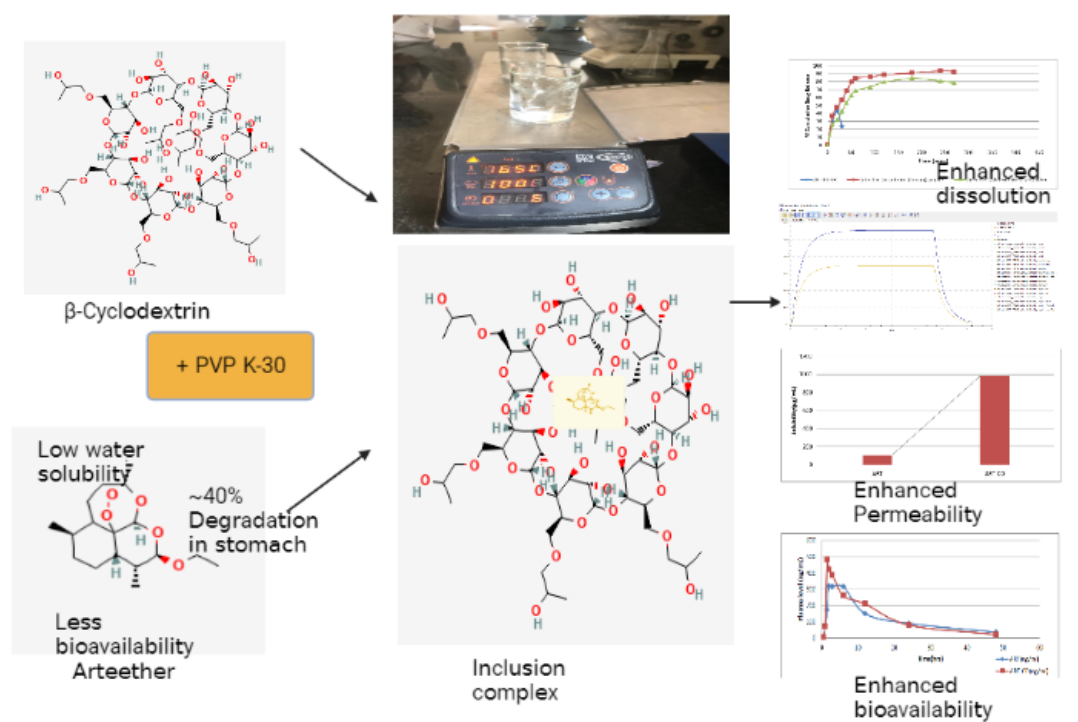


**Figure 4.3: Process of preparation of inclusion complex**

#### 4.4.3.4 Evaluation of CD inclusion complexes

Cyclodextrin complexes were evaluated and characterized by following methods:

##### 4.4.3.4.1 Percentage practical yield of ART-CD complex

The process' efficiency was determined by the practical yield achieved. The practical yield from CD complexes that were retrieved and measured was calculated using the equation 6

$$\text{Practical yield} = \frac{\text{Practical mass of inclusion complex}}{\text{Theoretical mass (drug+carrier)}} \times 100 \dots\dots\dots (6)$$

#### 4.4.3.4.2 Dissolution studies of ART-CD complex

Dissolution testing was performed using a USP dissolution rate test device in accordance with the standard methodology utilizing the UV technique (Boetker *et al.*, 2013). The dissolution investigations were carried out using the progressive dissolving method. Using a USP dissolving machine Type I and 750 mL 0.1N HCl as dissolution medium at 50 rpm at  $37 \pm 0.5^\circ\text{C}$ , all complexes were produced with the best feasible yield. The samples were withdrawn at 5, 10, 15, 20, 30, 45, and 60 min, and the volume was replaced with an equivalent amount of fresh dissolving medium. After 1.5 h, 125 mL of 0.1 N sodium hydrogen phosphate was added to the same solution to achieve a pH of 6.4. The absorbance was measured for 4 h. The samples were filtered and diluted. The absorbance of the resulting solutions was measured at 254 nm using a UV-visible spectrophotometer (Loftsson *et al.*, 2005). All measurements ( $n = 3$ ) were taken in triplicate.

#### 4.4.3.4.3 Drug content of ART-CD complex

In a volumetric flask of 50 mL, 100 mg of the complex was accurately weighed and dissolved in 40 mL of methanol. To get the solution up to volume, methanol was utilized. After diluting the solution with 0.1 N HCl, the drug concentration was measured at 254 nm using UV spectrophotometric analysis. All measurements ( $n = 3$ ) were taken in triplicate.

#### 4.4.3.4.4 Saturation solubility study of ART-CD complex

The saturated solution approach was used to determine the solubility of solid complexes. In a nutshell, 30 mg of ART— $\beta$ CD complex was suspended in 10 mL of aqueous phase and shaken at 100 rpm for 24 h at  $37 \pm 1^\circ\text{C}$  in an orbital incubator shaker. The suspension was then filtered, and 0.1 mL of it was dilute to 1 mL with water. The aliquot's contents were measured using the UV technique at 254 nm. All measurements ( $n = 3$ ) were taken in triplicate.

#### 4.4.3.4.5 Scanning electron microscopy (SEM) analysis of ART-CD complex

SEM (Jeol/JEM 2100) was used to examine the morphology of the solid inclusion complex. By producing a thin film on an aluminum stub, a sample of ART, ART— $\beta$ -CD, physical mixture (ART— $\beta$ -CD kneading 1:1 mM), and ART— $\beta$ -CD freeze

drying was studied. Under an argon environment, the stubs were subsequently coated with gold to a thickness of 200–500 microns. After that, the coated samples were evaluated and images were taken.

#### **4.4.3.4.6 Study of X-ray diffraction (XRD) of ART-CD complex**

The crystalline architecture of solid complex was determined using PXRD (Rigaku Corp., Japan) at a scanning rate of 1°/min spanning the 0–60° diffraction angle ( $2\theta$ ) range. ART, ART—CD complex PXRD pattern was obtained using Rotaflex, RV 200 powder XRD with Ni-filtered, Cu Ka-radiation, 40 mA current, and 40 kV voltage.

#### **4.4.3.4.7 Differential scanning calorimetry (DSC) of ART-CD complex**

Using a Differential Scanning Calorimeter, the synthesis of complex in solid state was also determined (DSC-7, Mettler Toledo). Under nitrogen purgation, the thermogram of an ART,  $\beta$ -CD physical combination, and an ART- $\beta$ -CD complex was collected at a rate of 10 °C/min (heating rate) throughout a temperature range of 30–260 °C.

### **4.5 Formulation development and characterization**

#### **4.5.1 Formulation development, optimization, and characterization of SLN**

##### **4.5.1.1 Risk assessment studies for preparation of SLNs**

The main objective of risk assessment was to identify the plausibility of risks/failures. To do so, the Ishikawa fish-bone diagram was constructed with the aid of Minitab 17 statistical software (M/s Minitab Inc., Philadelphia, PA) to depict a cause-effect relationship among the possible material attributes that were going to affect the critical quality attributes (CQAs) of the formulation. The obtained fishbone diagram depicted the influence of various process parameters and material specifications for the development of ART-loaded SLNs. Furthermore, a risk assessment matrix (RAM) was carried out for prioritization of selecting high-risk factors, to demonstrate the potential risks involved with different material specifications and process parameters of ART -SLNs on potential CQAs by designating a low, medium, and high-grade to each of the studied factors.

##### **4.5.1.2 Outlining Quality target product profile (QTPP) and CQAs for preparation of SLNs**

QTPP is a primary step towards QbD-oriented development of ART-SLNs, and is defined as ‘the imminent glossary of the quality attributes of a drug product that will

be achieved exemplary to ensure the desiderate quality, along with safety and efficacy of the drug product'. To meet the QTPP, various CQAs were identified such as particle size, and drug entrapment.

#### 4.5.1.3 Preparation of SLNs

ART-loaded SLNs were prepared by the spontaneous nanoprecipitation method with some modifications. Briefly, ART and stearic acid (6 mg) were dissolved in acetone/ethanol (1:1) mixture to obtain an organic phase. Then, the organic phase (was added dropwise using a syringe to 120 mL with 70°C temperature of the aqueous phase under continuous stirring at a magnetic stirrer for half an hour. The nanoparticle suspension was then lyophilized. The lyophilized SLN were then encapsulated in enteric coated capsule shells. The procedure is as shown in Fig 4.4.

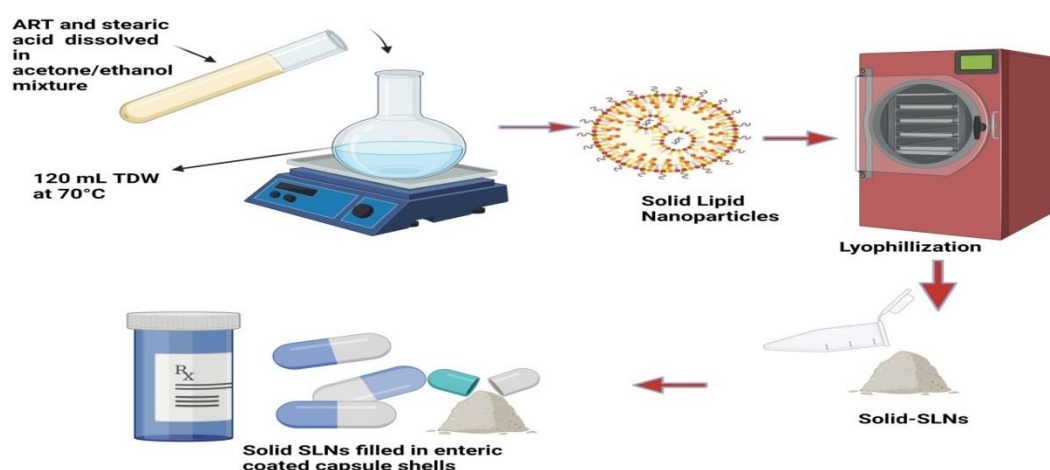


**Figure 4.4: Method of preparation of SLNs.**

#### 4.5.1.4 Optimization of SLNs by DoE

The randomized central composite design was employed to optimize ART-loaded SLN. Surfactant concentration and acetone to ethanol volume ratio in the organic phase were selected as independent variables. Particle size and % entrapment efficiency were selected as responses. The statistical analysis of the factorial design formulations was performed using Design-Expert® software (Version 13, Stat-Ease Inc.). Thirteen batches were prepared as suggested by the software using a central composite design with three levels, two factors, and two responses.



For optimization of these factors, Central Composite Design (CCD) was used with the help of Design Expert software. CCD was selected because of its capability to give a lesser number of experimental runs in comparison to other experimental designs.

Two factors i.e., concentration of surfactant and amount of organic phase were selected as the independent variable and CCD gave 13 experimental runs. Entrapment efficiency and particle size were selected as responses for the experimental runs. Table 4.8 shows the 13 experimental runs confirmed by CCD.

**Table 4.8: Experimental runs suggested by Central Composite Design.**

Run	A: Surfactant concentration (mg)	B: Organic phase (mL)
1	100	3
2	50	3
3	75	7.5
4	75	7.5
5	75	3
6	75	7.5
7	75	12
8	50	12
9	100	7.5
10	75	7.5
11	100	12
12	50	7.5
13	75	7.5

#### **4.5.1.5 Physicochemical characterization of ART-loaded SLNs**

##### **4.5.1.5.1 Particle size analysis and polydispersity index studies of ART-loaded SLNs**

Particle size and polydispersity index (PDI) of SLNs were determined by the Zeta sizer nano series (Malvern, USA). SLNs was subsequently redispersed in Milli-Q water and the particle size was recorded at 25 °C. All determinations were carried out in triplicates.

##### **4.5.1.5.2 Morphology of ART-loaded SLN**

Transmission electron microscopy (TEM) The particle shape of ART-loaded SLN was studied using TEM (FEI Tecnai F20, USA). One drop of the aqueous dispersion of SLN was loaded on the carbon-coated copper grid and was stained with a 2% w/v aqueous solution of phosphotungstic acid. The specimens were viewed under the microscope at an accelerating voltage of 120.0 kV.

#### **4.5.1.5.3 Entrapment efficiency (EE) of ART-loaded SLNs**

The nanoparticle dispersion was centrifuged for 15 min at 18,000 rpm using a centrifuge (Remi, India). From the supernatant, 0.1 mL was withdrawn and diluted up to 10 mL using methanol which was then analyzed using a UV spectrophotometer at 254 nm after acid degradation.

#### **4.5.1.5.4 Determination of Total Drug Content (TDC) of ART-loaded SLNs**

Similarly, for the estimation of TDC, SLN dispersion (1 mL) was disrupted using a suitable volume of chloroform: methanol mixture (2:1). The samples were vortexed to ensure complete extraction of the drug. The TDC was determined spectrophotometrically at  $\lambda_{\text{max}}$  of 254 nm. The studies were conducted in triplicate.

#### **4.5.1.5.5 Determination of pH of ART-loaded SLN**

The pH of SLNs was determined to check whether it will irritate oral administration or not.

The prepared ART-SLNs were lyophilized to make powdered SLNs which were further evaluated by different parameters. A variety of parameters, including size, shape, flow properties (Angle of repose, Hausner's ratio, and Carr's index), porosity, friability, disintegration time, drug content, and *in-vitro* drug release, were also assessed for the powdered SLNs.

#### **4.5.1.5.6 Particle size analysis of lyophilized ART-loaded SLNs**

The particle size of the powder SLNs was analysed by microscopic technique and was calculated directly by using a motic microscope.

#### **4.5.1.5.7 Flow properties of lyophilized solid ART-loaded SLN**

Hausner's ratio, compressibility index, and angle of repose may all be used to evaluate powder flow.

##### ***Angle of repose of lyophilized ART-loaded SLN***

The angle of repose was measured using the fixed funnel technique. A funnel was positioned above graph paper that was laid out horizontally and fastened with its tip at a certain height (h). The mixture was gently poured down the funnel until the conical pile's peak touched the funnel's tip. The conical pile's base's radius was calculated.

The angle of repose ( $\theta$ ) was calculated using the following equation:

$$\tan \theta = \frac{h}{r} \dots\dots\dots (5)$$

Where,  $\theta$  = Angle of repose,  $h$  = Height of the cone,  $r$  = Radius of the cone base. Values for angle of repose  $\leq 30^\circ$  usually indicate a free-flowing material and angles  $\geq 40^\circ$  suggest a poorly flowing material, 25- 30 shows excellent flow properties, 31-35 shows good flow properties, 36-40 show fair flow properties and 41-45 showing passable flow properties.

#### ***Carr's Index of lyophilized ART-loaded SLN***

The ability of a powder to be put into capsules is gauged by the Compressibility index (Carr's index) as given in Table 4.9. From the bulk and tapped densities, it is calculated. Theoretically, a material is more flowable if it is less compressible. As a result, it serves as a gauge for the relative significance of particle interactions. Such interactions are often less prominent in a free-flowing powder, and the values of the bulk and tapped densities will be closer. There are usually more particle interactions in poorly flowing materials, which results in a larger discrepancy between the bulk and tapped densities. These differences are reflected in the Carr's Index which is calculated using the following formula:

$$\text{Carr's index} = \frac{\rho_{\text{tap}} - \rho_b}{\rho_{\text{tap}}} \times 100 \dots\dots\dots (6)$$

Where,  $\rho_b$  = Bulk Density,  $\rho_{\text{tap}}$  = Tapped Density

**Table 4.9: Compressibility index values.**

<b>Compressibility Index (%)</b>	<b>Flow character</b>
$\leq 10$	Excellent
11 – 15	Good
16-20	Fair
21-25	Passable
26-31	Poor
32-37	Very poor
$>38$	Very Very poor

#### ***Hausner's ratio of lyophilized ART-loaded SLN***

The Hausner's ratio is a proximate indicator of powder flow simplicity. The formula used to compute it is as follows.

$$\text{Hausner's ratio} = \frac{t}{b} \dots\dots\dots (7)$$

where  $b$  is the bulk density and  $t$  is the tapped density. Hausner's ratios between 1.25 and 1.5 exhibit moderate flow qualities, while those above 1.5 suggest poor flow. Lower Hausner's ratios (1.25) imply better flow properties than higher ones.

#### ***Porosity of lyophilized ART-loaded SLN***

Lyophilized ART-loaded SLN percentage porosity was calculated using the following equation

$$\% \varepsilon = \frac{(\rho_t - \rho_b)}{\rho_b} \times 100 \quad \dots\dots (8)$$

Where  $\varepsilon$  = effective porosity,  $\rho_t$  = true density and  $\rho_b$  = bulk density.

#### ***4.5.1.5.8 In- vitro release studies of lyophilized ART-loaded SLN***

*In-vitro*, a drug release study of ART-SLNs was performed using the dialysis bag method. ART-SLNs (equivalent to 50 mg of ART) were dispersed in Milli-Q water and filled in a dialysis bag (Dialysis membrane, Hi media; MWCO 12,000e14,000 Da). The dialysis bag was closed from both sides and incubated in 250 mL of 0.1 N hydrochloric acid for the first 2 h followed by phosphate buffer pH 6.8 for the remaining period on a magnetic stirrer (50 rpm, 37 °C). Tween-80 (1%, w/v) was added to the release medium to maintain the sink condition during the dissolution study. Sample (2 mL) was withdrawn at pre-determined time points for 24 h and was replaced by an equal amount of fresh dissolution medium. Each sample after acid degradation was analysed by UV visible spectrophotometer at 254 nm. The study was carried out in triplicate.

#### ***4.5.2 Formulation development, optimization, and characterization of NLCs***

##### ***4.5.2.1 Risk assessment studies***

The main objective of risk assessment was to identify the plausibility of risks/failures. To do so, the Ishikawa fish-bone diagram was constructed with the aid of Minitab 17 statistical software (M/s Minitab Inc., Philadelphia, PA) to depict a cause-effect relationship among the possible material attributes that were going to affect the critical quality attributes (CQAs) of the formulation. The obtained fishbone diagram depicted the influence of various process parameters and material specifications for the development of ART-loaded NLCs. Furthermore, a risk assessment matrix (RAM) was carried out for prioritization of selecting high-risk factors, to demonstrate the potential risks involved with different material specifications and process parameters

of ART-loaded NLCs on potential CQAs by designating a low, medium, and high grade to each of the studied factors

#### 4.5.2.2 Outlining Quality target product profile (QTPP) and CQAs of NLCs

QTPP is a primary step towards QbD-oriented development of ART- NLCs, and is defined as ‘the imminent glossary of the quality attributes of a drug product that will be achieved exemplary to ensure the desiderate quality, along with safety and efficacy of the drug product’. To meet the QTPP, various CQAs were allocated such as particle size, and drug entrapment.

#### 4.5.2.3 Preparation of ART Loaded NLCs

The ART-NLCs was prepared by solvent diffusion method in an aqueous system as discussed in Fig 4.5. Briefly, ART, stearic acid (6 mg), oleic acid (6ml), and soya lecithin (3 mg) was taking in a test tube to make the organic solution. The resultant organic solution was quickly dispersed dropwise into 120 mL distilled water containing 1% Tween 80 under mechanical shaker (DC-40, Hangzhou Electrical Engineering Instruments, China) at 400 rpm in a water bath at 70°C for 5 min. The obtained pre-emulsion (melted lipid droplet) was then cooled at 27 °C $\pm$  2 °C till drug-loaded NLC dispersion was obtained. The milky white NLCs were further used for characterization. The prepared NLCs were then lyophilized to make solid powdered NLCs which were then filled in enteric coated capsule shells.

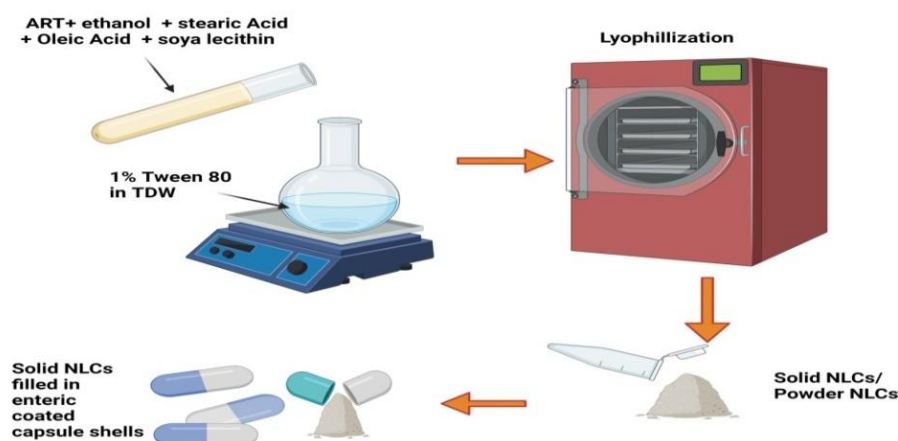


Figure 4.5: Method of preparation of NLCs.

#### 4.5.2.4 Central Composite Design (CCD) for systematic optimization of NLCs

CCD with alpha unity was applied on two factors selected i.e., lipid concentration and Surfactant concentration. The different factor combinations generated as per  $3^2$  factorial face-centered design are represented in Table 4.10. This design includes 13 experimental runs with 8 axial and 5 center points. The CQAs selected were particle size and Entrapment efficiency. Design Expert® software (version 13, Stat-Ease Inc. Minneapolis, USA) was used for constructing the design making and analyzing the results with the help of suitable mathematical models. The 2-D contour graphs and 3-D response surface graphs were constructed with the aid of software. The simultaneous graphical optimization approach was selected to locate the optimized formulation within the design space.

**Table 4.10: Design matrix for screening of factors as per CCD.**

Std	Run	A:Surfactant Concentration (mg)	B:Lipid Concentration (mg)
6	1	150	100
3	2	50	150
10	3	100	100
4	4	150	150
11	5	100	100
1	6	50	50
12	7	100	100
8	8	100	150
5	9	50	100
9	10	100	100
2	11	150	50
13	12	100	100
7	13	100	50

#### 4.5.2.5 Characterization of optimized NLCs containing ART

##### 4.5.2.5.1 Particle size, zeta potential, and PDI (polydispersity index) of NLCs

The particle size, zeta potential, and PDI of the developed NLC formulations were examined. Samples were housed in a polystyrene cuvette and observed at a fixed angle of 90 degrees at a temperature of  $25 \pm 0.1^\circ\text{C}$  after diluting 10 times with distilled water. At  $25 \pm 0.1^\circ\text{C}$ , laser Doppler anemometry was utilised to calculate the zeta potential of NLCs. In an electrophoretic cell with a 15.24 V/cm electric field, undiluted samples were kept (Cunha *et al.*, 2020).

##### 4.5.2.5.2 Evaluation of surface topography of NLCs

The surface topography of the prepared NLCs was examined using TEM. On a colonial grid covered with a membrane surface, a diluted drop of NLC solution was put, and 1 % phosphotungstic acid was added immediately. The extra fluid was removed after 1–2 min, and the grid's surface was air-dried at room temperature before being studied (Beg *et al.*, 2018).

The samples are frozen to  $-30\text{ }^{\circ}\text{C}$  for 12 hours resulting in the sublimation of phage particles and secondary drying step results in the desorption of remaining water molecules (from  $-30\text{ }^{\circ}\text{C}$  to  $25\text{ }^{\circ}\text{C}$  for 10 hours), leaving the dry lyophilized powder.

A variety of factors, including size, shape, flow properties (angle of repose, hausner's ratio, and Carr's index), porosity, friability, disintegration time, drug content, and *in-vitro* drug release, were assessed for the optimised formulation after lyophilization.

#### **4.5.2.5.3 Flow properties of lyophilized NLCs**

Hausner's ratio, compressibility index, and angle of repose may all be used to evaluate powder flow.

All the parameters evaluated for flow properties of powder NLCs were determined as discussed in section 4.5.1.5.7 (*Flow properties of SLNs*).

#### **4.5.2.5.4 Drug entrapped and drug loading of ART loaded NLCs**

The direct lysis approach was used to determine drug loading efficiency and drug entrapment. In an ultracentrifuge, the measured quantity (20 mL) of NLCs was centrifuged for 20 min at 40,000 rpm ( $4^{\circ}\text{C}$ ) (Gurumukhi *et al.*, 2021). The pellet was washed three times in DDW to eliminate any drug that had become entrapped after the supernatant was extracted. The particle was then extracted and lysed in chloroform. After that, the lysed samples were diluted in methanol and passed through 0.22 mm filters. The drug concentration in the filtrate was determined in triplicate using UV spectroscopy at 254 nm after acid degradation. .

#### **4.5.2.5.5 Drug release studies of ART loaded NLCs.**

The dialysis bag diffusion method was used to produce *in vitro* medication release. The NLC dispersion (5 mL) was deposited in a dialysis membrane knotted on both sides (MWCO10–12 kDa, Himedia, India) in a 20 mL solvent combination of PBS (pH = 6.8) and ethanol (70:30, v/v). The beakers were then held at  $32\text{ }^{\circ}\text{C}$  for incessant stirring on a magnetic stirrer at 50 revolutions per minute (Gurumukhi *et al.*, 2021).

One mL of sample was withdrawn from the beaker at predetermined time intervals and replaced with the same amount of release media. The samples were then subjected to UV spectroscopic analysis at 254 nm after acidic degradation.

#### ***4.5.3 Self micro emulsifying drug delivery system (SMEDDS)***

##### ***4.5.3.1 Formulation Optimization and Development of SMEDDS***

###### ***4.5.3.1.1 Risk assessment studies of SMEDDS***

Risk assessment's primary purpose was to determine the credibility of failures and risks. An Ishikawa fishbone diagram was created using Minitab 17 statistical software (M/s Minitab Inc., Philadelphia, PA) to represent the cause and effect link between the potential material qualities that might impact the formulation's key quality attributes (CQAs). The resulting fishbone diagram established the effect of several process parameters and material specifications on the production of ART-SMEDDS. Additionally, a risk assessment matrix (RAM) was used for prioritizing the selection of high-risk factors to establish the potential hazards associated with materials and process parameters for ART loaded SMEDDS on potential CQAs by assigning a high, medium, or low-risk level to each of the factors studied.

###### ***4.5.3.1.2 Outlining Quality Target Product Profile (QTPP) and CQAs of SMEDDS***

QTPP is a critical stage in the QbD-oriented development of ART- SMEDDS. To comply with the QTPP, numerous CQAs were assigned, including particle size and drug entrapment. The QTPP elements and CQAs for products/processes impacting the performance of ART-SMEDDS are listed in Table 4.10

###### ***4.5.3.1.3 CMA for development of SMEDDS***

"Material attributes" refers to the material's physical, chemical, biological, or microbiological qualities. The raw material, active pharmaceutical substances, solvents, reagents, and process aids utilized in manufacturing medicines may all be input materials. As a result, CMAs include lipids, surfactants, and cosurfactants, which must be accounted for in the DoE. Simultaneously, the highest priority should be identifying acceptable excipients for formulation development through DoE.



#### 4.5.3.1.4 CPP for development of SMEDDS

CPPs comprise variables relating to processes affecting the quality of the final product. To ensure that the product meets established specifications, all production processes must be scrutinized and managed during the preparation process. SMEDDS was prepared by combining the API with a preconcentrate of oil, cosurfactant, and surfactant combination. The CPPs used in SMEDDS preparation include temperature, stirring time, and speed used throughout the preparation. Fig 4.6 shows the primary elements of risk assessment.

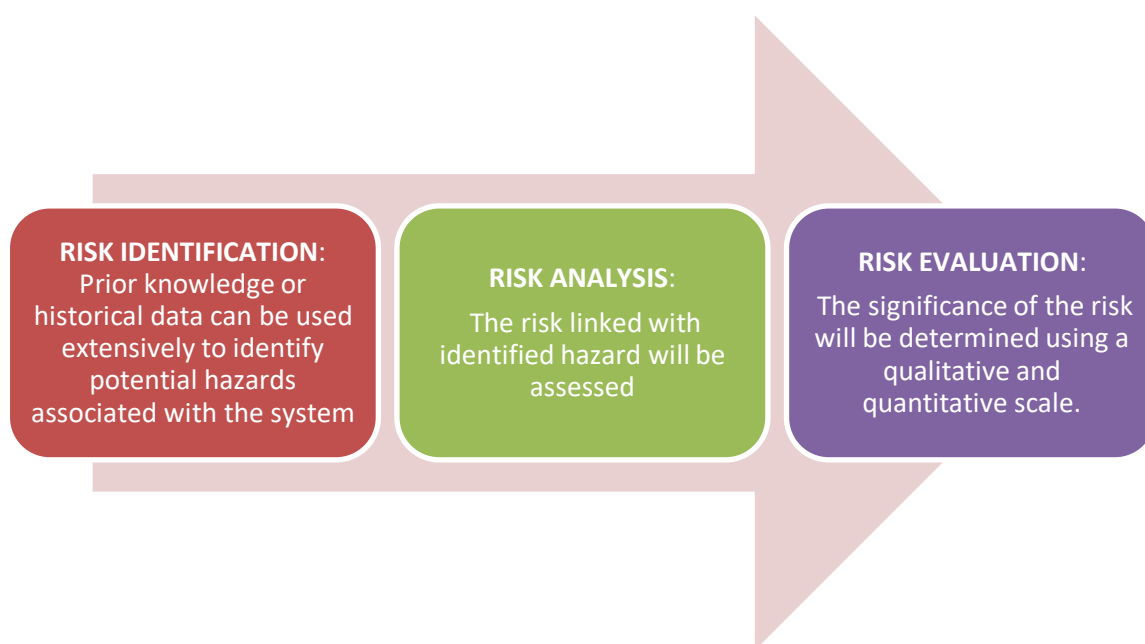


**Figure 4.6: Major elements of risk assessment during development of SMEDDS.**

#### 4.5.3.2 Formulation development, optimization, and characterization of SMEDDS

##### 4.5.3.2.1 Equilibrium solubility studies of ART

The shake flask technique was utilized for the measurement of the equilibrium solubility of ART in a variety of pH buffers (1.2, 4.5, 6.8, 7.4, and pure water.) (Greenwood *et al.*, 2008). An adequate quantity of ART powder was added to screw cap vials (5 mL) containing buffer solutions (3 mL). Vials containing ART were shaken at 100 rpm for about 6 h at  $37 \pm 0.5^\circ\text{C}$ . Afterward, the answer was subjected to centrifugation for 10 min at 15000 rpm at  $25^\circ\text{C}$ , then filtered the supernatant using 0.45 m filter paper. Further analysis of the acquired sample was performed using HPLC at a fixed wavelength of 214 nm.

#### **4.5.3.2.2 Constituents of SMEDDS**

##### **4.5.3.2.2.1 Solubility studies for screening of ART in oil**

ART's solubility was evaluated separately in various oils, cosurfactants, and surfactants using the shake flask method. ART was added in excess amount in 2 mL of the component. The sample was blended using a vortexer (GeNei, Bangalore, India) for 5 min. Subsequently, the shaker bath (Tempo Instruments and Equipments Pvt. Ltd., Mumbai, India) was employed at 37°C for 72 hours temperature at 300 rpm. Following equilibrium for another 72 h at 25°C, every vial was subjected to centrifugation at 10000 rpm for 1 min utilizing a centrifuge (Remi Laboratory Instruments, Mumbai, India). Then solution filtration was achieved using a membrane filter (0.45 µm) to remove ART remaining. The quantity of ART in every sample was assessed through a dual-beam UV Visible spectrophotometer at 254 nm after acid degradation. The drug experiment was conducted thrice, and the average results were noted for further studies (Kumar & Mishra, 2006).

##### **4.5.3.2.2.2 Surfactant screening through emulsification of ART**

Different non-ionic surfactants (Span 80, Span 20, Tween 80, Tween 20 and PEG 400) were investigated. The applicable limits were applied to the selection of surfactants dependent on their role in the product (Loh *et al.*, 2016). The experiment was replicated three times, and the mean statistics were obtained.

##### **4.5.3.2.2.3 Emulsification of the maximal oil quantity possible**

In distilled water, 10 mL of each surfactant's 10% w/v solution was created. Each of these solutions was mixed with previously adjusted oil in increments of 10 mL and vortexed till it became hazy (Dwivedi *et al.*, 2015). They investigated the ability to retain transparency at a higher proportion and emulsification ease. Every surfactant was mixed in the oil phase in separate glass vials in optimum 1:1 ratios. All of these combinations were gently boiled at 50°C using a water bath to homogenize the components. Each of the mixtures mentioned above was diluted 1000 times in a volumetric flask using distilled water. The emulsification ease was assessed through the frequency of inversion of the flask necessary to obtain a homogenous emulsion. Additionally, each emulsion sample was left at rest for 2 hours before being tested individually for percentage transmittance (% T) at 254 nm using a UV

spectrophotometer. Additionally, the formulations were tested visually for phase separation and transparency after storage at 25°C for 24 hours.

#### **4.5.3.2.2.4 *Cosurfactant screening through emulsification***

Five cosurfactants (PEG 400, Span 20, Tween 20, dichloromethane, Tween 80) were assessed for the capacity in aiding the emulsification of the respective oil phase when employed in combination with the previously chosen surfactant. The cosurfactant screening was undertaken to engage constraints based on their role in the dosage form. The experiment was repeated three times, and the mean statistics were obtained.

#### **4.5.3.2.2.5 *Emulsification of the maximal oil quantity dissolves with both surfactant and cosurfactant***

Cosurfactant and surfactant (1:1) were employed to form 10% solution (w/v) using 10 mL distilled water. Each of these solutions was mixed with previously adjusted oil in increments of 10 mL and vortexed until the system became hazy.

The cosurfactant was adjusted 1:1:2 with the optimal surfactant and oil phases. Additionally, the mixtures were treated as outlined in surfactant optimization as well as metrics such as % T and ease of emulsification were recorded (Daily, 2006).

#### **4.5.3.2.3 *Construction of ternary phase diagram for preparation of SMEDDS***

By constructing ternary phase diagrams, it was determined that self-micro emulsifying formulations exist which can emulsify with mild agitating. After preliminary optimization, components such as oil, cosurfactant, and surfactants were used as the triangle's apex phase diagram. Several self-micro emulsifying systems (SMEDDS) were produced with a set dosage in every conceivable ratio of all the components (0-100%). For each dosage form, 0.5 ml was added 500 mL 0.1N HCl at 35-37°C, and the mixture was gently swirled at 50 rpm through a magnetic stirrer (Remi Laboratory Instruments, Mumbai, India). Additionally, a particle size analyzer (Zetatrac, U2552, NY) was utilized to assess all prepared formulations' globule size and size distribution. Ternary phase diagrams were created by detecting formulations with globule sizes more fabulous than 5100 nm by employing a demo version of TriplotV14 software (Choksi *et al.*, 2007).

#### 4.5.3.2.4 Drug-excipients compatibility studies for preparation of SMEDDS

In SMEDDS, the drug is in intimate contact with one or even more excipients, which might impair the drug's stability. Compatibility data between drugs and excipients are thus precious for formulators when choosing acceptable excipients. As a result, the ART was maintained in a sealed container with the excipients for the specified length of time, and then its qualities were checked. The drug excipient compatibility are discussed in (section 5.4.3.1.2) The appropriate excipient was chosen due to its excellent solubility and compatibility with the medication.

#### 4.5.3.3 SMEDDS development

At ambient temperature, various SMEDDS were prepared by dissolving ART in arachis oil and mixing surfactants (tween 80) and co-surfactants (span 20) in optimised ratio. The completed mixture was vortexed for 30 minutes to ensure thorough mixing and the formation of a clear solution. The SMEDDS were tested for phase separation and turbidity, equilibrated, and kept at room temperature.

SMEDDS were analyzed in gastric intestinal fluid when they came into direct contact with various physiological fluids. No change in colour was detected when GI fluid was added, and no turbidity was observed when 900 mL of water was added. The prepared SMEDDS were adsorbed on the surface of colloidal silica and were filled in enteric coated capsule shells for oral delivery as shown in Fig. 4.7.

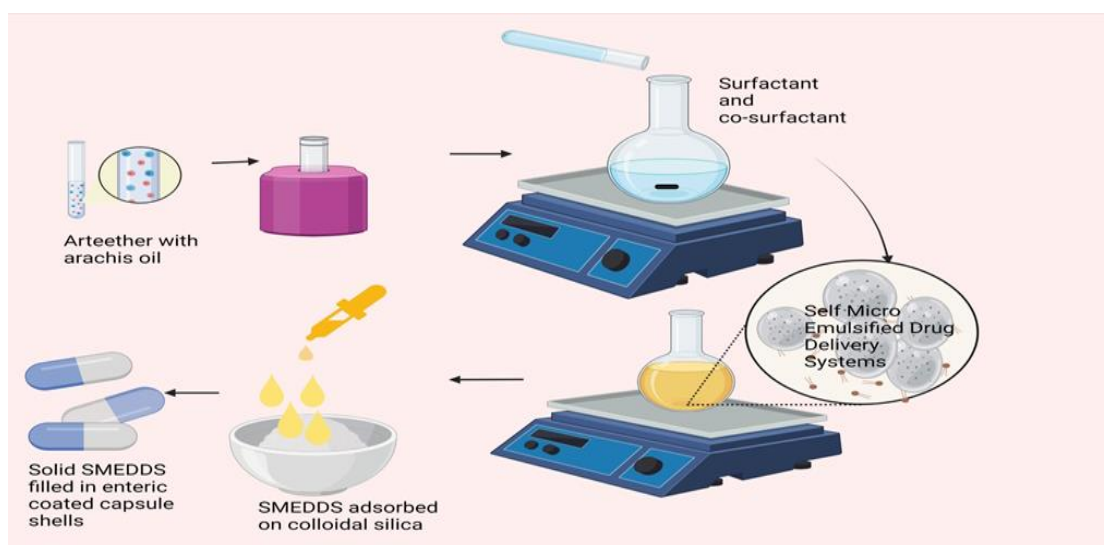


**Figure 4.7: Method of preparation of SMEDDS.**

#### 4.5.3.3.1 Selection of design for SMEDDS

Arachis oil, Tween-80, and Span-80 were selected as main three components of the formulation combination, and the proportions of all three ingredients directly affect the formulation's content uniformity. Additionally, the ranges of all three elements are distinct from one another. Hence Optimal Constrained Mixture Design was used to optimize the ratio of all three components in SMEDDS formulation. After defining the ranges for all three components, data on the average assay and % RSD are collected in all 16 experimental runs of the specified design. Table 4.11 shows the three components used for the preparation of SMEDDS.

**Table 4.11: Components for the preparation of SMEDDS.**

Run	A:Arachis oil	B:Tween 80	C:Span 80
	%	%	%
1	73.7	10.0	16.3
2	73.7	10.0	16.3
3	61.9	13.1	25.0
4	66.7	15.5	17.8
5	75.1	14.6	10.3
6	60.0	30.0	10.0
7	61.9	13.1	25.0
8	65.0	30.0	5.0
9	69.7	20.0	10.4
10	75.0	19.9	5.2
11	69.7	20.0	10.4
12	60.0	25.0	15.0
13	80.0	15.0	5.0
14	60.0	25.0	15.0
15	70.0	25.0	5.0
16	69.7	20.0	10.4

#### 4.5.3.3.2 Visual evaluation of SMEDDS

Visual examination of self-emulsification is feasible. The opaque and milky white appearance of SMEDDS after dilution with water implies macroemulsion production, while the clear, isotropic, transparent solution shows microemulsion formation. Visual

examination of drug precipitation in diluted SMEDDS is also feasible. When no evidence of drug precipitation is seen, the formulations may be termed stable. Precipitation is a frequent occurrence in formulations that include hydrophilic cosolvents and may be prevented by raising the surfactant content.

#### **4.5.3.3.3 Size of globules and zeta potential of SMEDDS**

The dimensions of SMEDDS droplets were estimated through a Zeta sizer Nano ZS model (Malvern Instruments), while Laser doppler anemometry (Malvern Zetasizer) was utilized to measure measurement zeta potential. Before assessing the zeta potential, all SMEDDS were diluted 100 times with TDW to an adequate concentration. Triplicate measurements were made in a completely automated mode.

The prepared SMEDDS were then adsorbed on the surface of colloidal silica to solidify them. The solidified SMEDDS were further evaluated. A variety of factors, including size, shape, flow properties (Angle of repose, Hausner's ratio, and Carr's index), drug content, and in-vitro drug release, were assessed for the optimised formulation.

All the parameters evaluated for flow properties of powdered SMEDDS are as discussed in section 4.5.1.5.7 (*Flow properties of SLNs*).

#### **4.5.3.3.4 Determination of percentage drug entrapped of SMEDDS**

To determine PDE, the vesicles were maintained at 4°C overnight, followed by ultracentrifuged at 35,000 rpm for 3 h at 4°C (Rahman *et al.*, 2016). The supernatant was extracted, and the drug concentrations in the sediment and supernatant were determined. The silt was solubilized using methanol, and the quantity of ART entrapped was measured in triplicate spectrophotometrically at  $\lambda_{\text{max}}$  of 254 nm.

#### **4.5.3.3.5 High-resolution Transmission Electron Microscopy (HR-TEM)**

SMEDDS were diluted as well as characterized using HR-TEM (Tecnai™ G2 F20, Eindhoven, The Netherlands) at 210 kV acceleration voltage

#### **4.5.3.3.6 Determination of Total Drug Content (TDC)**

Similarly, to determine TDC, a 1 mL dispersion of SMEDDS was disrupted with an appropriate proportion of chloroform: methanol combination (2:1). Vortexed samples were used to achieve complete drug extraction. At  $\lambda_{\text{max}}$  of 254 nm the TDC was calculated spectrophotometrically after acid degradation. The studies were replicated three times. TDC was determined.

#### **4.5.3.3.7 Determination of pH of prepared SMEDDS**

The pH was analysed using a glass electrode pH meter (Labindia Picop, Mumbai, India).

#### **4.5.3.3.8 Determination of drug release (%) of SMEDDS**

A dialysis bag approach was followed to examine the release of ART-SMEDDS. ART-SMEDDS (equal to 50 mg of ART) was dispersed in Milli-Q water and added to the dialysis bag. The dialysis bag from both ends was sealed and incubated for the first 2 h in 250 mL of 0.1 N HCl, followed by the remainder of the period in phosphate buffer pH 6.8 with a magnetic stirrer (50 rpm, 37°C). Tween-80 (1% w/v) was introduced in the media during the dissolution trial to maintain the sink condition. For 24 h, 2 mL of the sample was collected and substituted with an equivalent quantity of new media at fixed time intervals. After acid destruction, each piece was examined using a UV-visible spectrophotometer set at 254 nm. The study was replicated three times.

#### **4.5.3.3.9 Thermodynamic stability studies/stability under centrifugation of SMEDDS**

Microemulsion shows centrifugation resistance dependent on the density gradient between the aqueous and oil phases and interfacial coating resistance. Thus, for formulations with very comparable densities, the stability under centrifugation is proportional to the strength of the interfacial coating. This investigation used 10 mL of formulation for centrifugation for 30 min at 3500 rpm (Goindi *et al.*, 2013). A freeze/thaw cycle was performed on hermetically sealed test tubes containing the prepared formulation. The test tubes were vertically placed in the freezer at 21°C for 16 h and subsequently at 27 °C±2 °C for 8 h. If there is any change in the formulation was noted and the experiment was carried out four times.

#### **4.5.3.3.10 Preparation of encapsulation of solid SMEDDS in enteric-coated capsule shells**

Solid SMEDDS were made by adsorbing a set quantity of ART-SMEDDS (30%) onto silicon dioxide (10%) until the liquid ART-SMEDDS was entirely adsorbed.

The homogeneity of the drug content in the prepared solid SMEDDS was determined. In a 10 ml volumetric flask, a sample of 640 mg was collected. The solid SMEDDS

were then encapsulated in enteric coated capsule shells and further used for *in vivo* studies.

#### 4.5.4 Formulation development, optimization, and characterization of CD complex spheroids encapsulated in enteric capsule shells

Spheroids were prepared by the extrusion-spheronization process as shown in Fig. 4.8. ART-CD Spheroids were prepared by using polyvinyl pyrrolidone (PVP) K 30 as a binder, sodium starch glycolate as a disintegrant, and microcrystalline cellulose (MCC or Avicel 101) as filler. As the drug is slightly gummy so colloidal silica is also added to the mixture. All the ingredients were accurately weighed and blended with the required quantity of the drug. Then ethanol was added to the blended ingredients to form a wet mass or dough. When this dough was passed through an extruder; cylindrical-shaped extrudates were formed. The extrudates were collected in a spheronizer for rounding the extrudates. The formed spheroids were optimized based on spheronization time, shape, concentration of binder, and disintegrant. The prepared spheroids were filled in enteric-coated capsules.

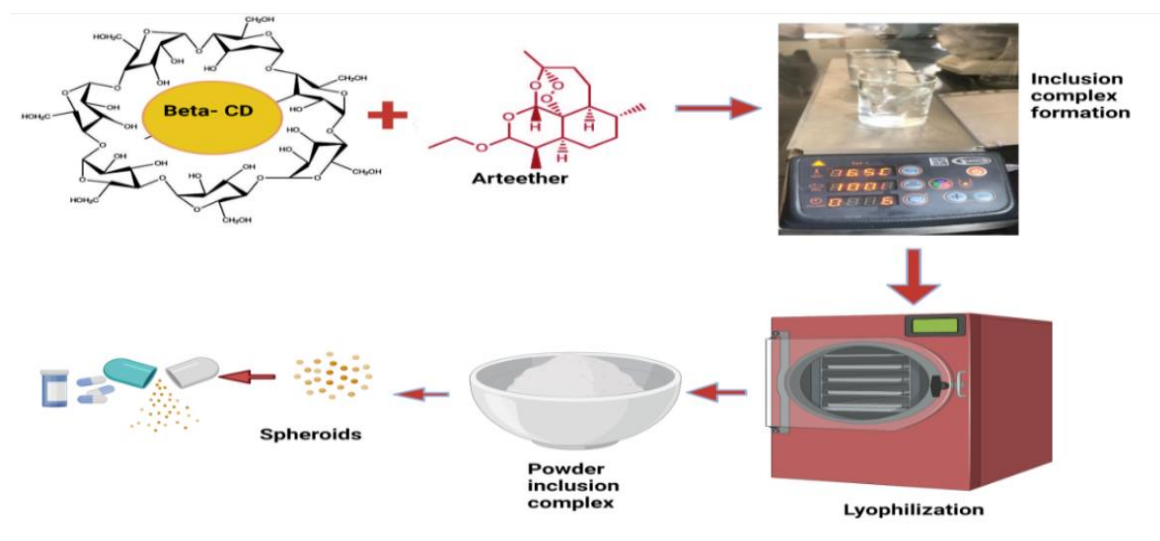


**Figure 4.8: Method of preparation of spheroids.**

##### 4.5.4.1 Evaluation of spheroids preparation parameters of CD inclusion complexes

Flow properties, such as angle of repose, poured density, tapped density, and compressibility index of inclusion complexes, were measured according to Ph. Eur.<sup>7th</sup> Ed.



#### 4.5.4.2 QbD based analysis for the optimization development of spheroids

Based on the previous analysis of literature and brainstorming discussion among the research team, various critical factors that can affect the final quality parameters of spheroid were identified. Parameters such as stirring time, stirring speed, disintegration concentration, and binder concentration were considered critical ones that can affect the final quality parameters.

Therefore for optimizing the 4 factors at a time, 4 levels of Box Behnken Design (BBD) was applied. BBD was created using the Design Expert software version 13(State-Ease Inc, USA). Four critical factors i.e., stirring time, stirring speed, disintegration concentration, and binder concentration were selected as independent variables, and dissolution (%) was selected as the response or dependent variable. BBD for 4 factors gave 29 runs as shown in Table 4.12. The DoE was not only employed in this study for the determination of the optimized value of the selected critical variables but it can also give the correlation between the selected independent variables with that of dependent variables. The RSM was employed for creating a non-linear quadratic model, which possibly depicted the relationship between the independent and dependent variables with the model equation as follows:

$$Y = b_0 + b_1A + b_2B + b_3C + b_4D + b_5AB + b_6AC + b_7AD + b_8BC + b_9BD + b_{10}CD + b_{11}A^2 + b_{12}B^2 + b_{13}C^2 + b_{14}D^2 \dots\dots\dots(9)$$

Where Y is a response,  $b_0$  is the intercept, and  $b_1$ -  $b_{13}$  are the regression coefficients of different factors and their quadratic polynomials.

**Table 4.12: Experimental runs created by BBD for optimization of critical factors for spheroids.**

Run	A: Stirring speed	B: Stirring time	C: Disintegration concentration	D: Binder concentration
	(rpm)	(min)	(mg)	(mg)
1	700	7	100	150
2	500	7	50	150
3	700	5	50	150
4	900	9	150	200
5	700	5	150	150
6	700	5	100	200
7	500	9	100	150
8	900	7	50	150
9	700	9	100	200
10	500	5	100	150
11	500	7	100	200
12	700	9	50	150
13	700	7	150	100
14	700	7	100	150
15	700	7	100	150
16	500	7	150	150
17	700	7	50	100
18	700	7	150	200
19	500	7	100	100
20	700	5	100	100
21	900	7	100	100
22	900	7	150	150
23	700	7	100	150
24	900	8	150	200
25	700	7	100	150
26	700	7	50	200
27	900	9	175	200
28	700	9	200	100
29	700	9	150	150

#### 4.5.4.3 Physicochemical characterization of optimized formulation of ART-CD spheroids

Various physico-chemical parameters of spheroids like shape, spheroid size, and size distribution, friability, drug content, flow properties, were measured according to Ph. Eur. 7<sup>th</sup> Ed. while disintegration time and *in vitro* drug release are discussed as follows.

##### 4.5.4.3.1 Flow properties of ART-CD spheroids

Measurements of the bulk density, tapped density, Hausner's ratio, and Carr's index in triplicate using conventional techniques were used to examine the flow characteristics of enteric-coated spheroids.

The flow properties of prepared Spheroids were determined as discussed in section (4.5.1.3.5) i.e. (*Flow properties of SLNs*).

##### **Bulk density of ART-CD spheroids**

The mass of the powder divided by the bulk volume is known as bulk density. Particle form has a significant impact on bulk density; as particles grow more spherical, bulk density rises. By pouring spheroids into a graduated cylinder and weighing and measuring the volume of the pellets, the bulk density of the coated spheroids was measured using following formula.

$$\text{Bulk density} = \frac{\text{weight of spheroids}}{\text{Bulk volume of spheroids}} \dots\dots\dots (10)$$

##### **Tapped density of ART-CD spheroids**

By putting a graduated cylinder with a given quantity of spheroids and adjusting the cylinder in mechanical tapper equipment, the tapped density was ascertained. The machine was run for a predetermined number of taps until the powder bed volume was at a minimum. The density of the minimal volume tapped was estimated using the weight of the medication in the cylinder.

$$\text{Tapped density} = \frac{\text{weight of spheroids}}{\text{Tapped volume of spheroids}} \dots\dots\dots (11)$$

##### 4.5.4.3.2 Disintegration time from ART-CD spheroids

The spheroids disintegration was evaluated by a tablet disintegration tester (Singhla Scientific, India). A transparent tube of 10 mm diameter and 15 mm length was used. Sieves of 2 ±0.2 mm mesh size were at the top and the bottom of this tube. After filling 100 mg of pellets in each tube, they were inserted in the standard tablet

disintegration tester. The disintegration of spheroids was calculated initially in 0.1 N HCl for 2 hrs and then in PBS pH 6.8 for 1 hr. The disintegration time of six dried samples at  $37 \pm 0.5^\circ \text{C}$  was determined at a speed of 30 dips.

#### **4.5.4.3.3 *In vitro* drug release from ART-CD spheroids**

The dissolution studies of enteric-coated encapsulated spheroids containing cyclodextrin complexed ART were carried out according to the USP II paddle apparatus. For drug release studies of the enteric coated encapsulated spheroids, 0.1 N HCl (900 mL) was used as a dissolution medium for the first 2 h and then it was replaced by phosphate buffer pH 6.8 (900 mL). Spheroids (100 mg) were immersed in the dissolution medium and were maintained at  $37 \pm 0.5^\circ \text{C}$  and stirred at 100 rpm. At definite time intervals, 5 mL of the aliquots of the sample was withdrawn periodically and the volume was replaced by an equivalent amount of dissolution medium to maintain the sink conditions. The samples were analyzed spectrophotometrically after acid degradation at 254 nm for phosphate buffer using a UV- spectrophotometer.

#### ***Evaluation parameters for enteric coated capsule shells***

Prepared lyophilized SLNs, NLCs, SMEDDS and spheroids were filled in enteric coated capsule shell, purchased from Purecapsusa (size 0). The capsule shells filled with formulations were evaluated on the basis of weight loss/gain, visual aspect, brittleness, weight variation, moisture content.

#### **4.5.5 *Enteric-coated tablets***

##### **4.5.5.1 *Quality profiling and identification of QTPP, CQAs, and CPPs of enteric coated tablets***

The most important and first stage in developing a patient compliance dosage form is determining different quality features of the formulations to be generated for defining QTPP. The aesthetic aspect of oral formulations is very important in terms of adoption. The quality attributes linked to the product's safety and effectiveness are defined by the FDA as QTPP. Route of administration, dosage form, delivery methods, dose strength(s), container closing mechanism, pharmacokinetic considerations, and drug product quality requirements may all be included (e.g., sterility, purity, stability, and drug release). "A physical, chemical, biological, or microbiological property or feature that should be within a suitable limit, range, or distribution to provide the intended product quality," according to the definition of a

CQA. QTPP features including assay, content uniformity, dissolution, and permeation flux, on the other hand, were included in CQA since they can be affected by formulation or process factors.

#### **4.5.5.2 Risk assessment of enteric coated tablets**

Implementation of risk assessment strategies is critical to get insights on potential high risks and to develop the risk management protocols to ascertain the product of desired quality. Assessment of risk was done to recognize all the potential high-hazard factors which will be exposed to a DoE study to set up the design space. According to ICHQ9 guidelines, risk identification and risk analysis are the two most important factors for risk assessment. Risk identification was done by constructing Ishikawa fishbone diagram that illustrates all potential factors that have some impact on the quality of the enteric-coated tablet. The second step of risk assessment i.e., risk analysis was done by employing the Hazard Analysis and Critical Control Points (HACCP) method (Imig *et al.*, 2022). (Bhoop, 2014) provided a detailed analysis of the HACCP method to understand the hazard in the processes including both the safety and quality parameters of the product and process involved in the manufacturing (Angus *et al.*, 1997). In the present study, after initial risk assessment, identified risks were ranked based on two criteria evaluation methods in which identified potential risks were ranked on the scale of three categories “Low Risk”, “Medium Risk” and “High Risk”. Low-risk categories consist of all those risks that have very less impact on the quality of the product. Medium risk contains the risk that has a moderate impact and those risks which have the greatest impact on the quality of the product was categorized in the “High risk” category. This risk estimation matrix targets to identify and rank formulations and process variables based on their degree of risk for quality failure. This will further help in identifying the most critical quality parameters for the optimization of product-employed designed experimentation (Devane, 1998).

#### **4.5.5.3 Formulation development, optimization, and characterization of enteric-coated tablets**

Enteric-coated tablets were formulated using starch paste (10 %) as the binder. Enteric-coated tablets of ART were prepared by wet granulation process. Accurately weighed quantities of drug, filler (lactose), and microcrystalline cellulose as an anti-adherent were mixed in a mortar. The required quantity of binder (starch in water as

10% solution) was added and the same was mixed thoroughly to form a mass suitable for granulation. The dough mass was then passed through sieve # 22 to form granules which were dried in an oven at 120° for 20 min. The granules were mixed with the required quantities of lubricant (talc) and glidant (magnesium stearate), which reduces friction between the tablet and the walls of the die cavity along with the stickiness of the tablet to the die and punch. The mixture was then compressed to form tablets in a single-station rotary tablet machine using 10 mm round concave punches at optimum pressure as shown in Fig. 4.9. Coating of the polymer (Eudragit S100) was done in a rotating drum coating device. A 6% w/v polymer solution was used for the core coating.

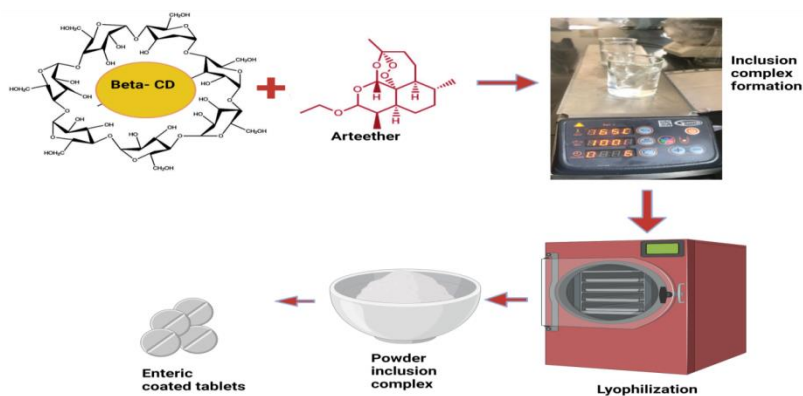


**Figure 4.9: Method of preparation of enteric-coated tablets.**

To prevent drug degradation in the acidic environment of the stomach, tablets of  $\alpha$ ,  $\beta$ -ART were enteric coated using eudragit S100 polymer in a rotating drum coating device. A batch of 100 tablets was coated. The coated solution was prepared by dissolving eudragit S100 polymer (6% w/v) in isopropyl alcohol (IPA) and kept stirring under mechanical stirring for 2-4 hrs. After that solution was plasticized with propylene glycol and lubricated with talc 2% w/v and the final volume was made up to 100% with IPA and then again kept for stirring under mechanical stirring for 1-2 hrs. The process conditions were pre-warming cores at 40°C for 10 min. Under these conditions (spray nozzle diameter 1 mm; atomizing air pressure 1 bar air flow rate 80 m<sup>3</sup>h<sup>-1</sup> inlet air temperature 40°C, product temperature 32-35°C; spray rate 1.5 mL/min, spraying nozzle set on a distance of 10 cm, post drying at 40 °C for 10 min.) The method of preparation of enteric-coated tablets has been shown in Fig. 4.10.

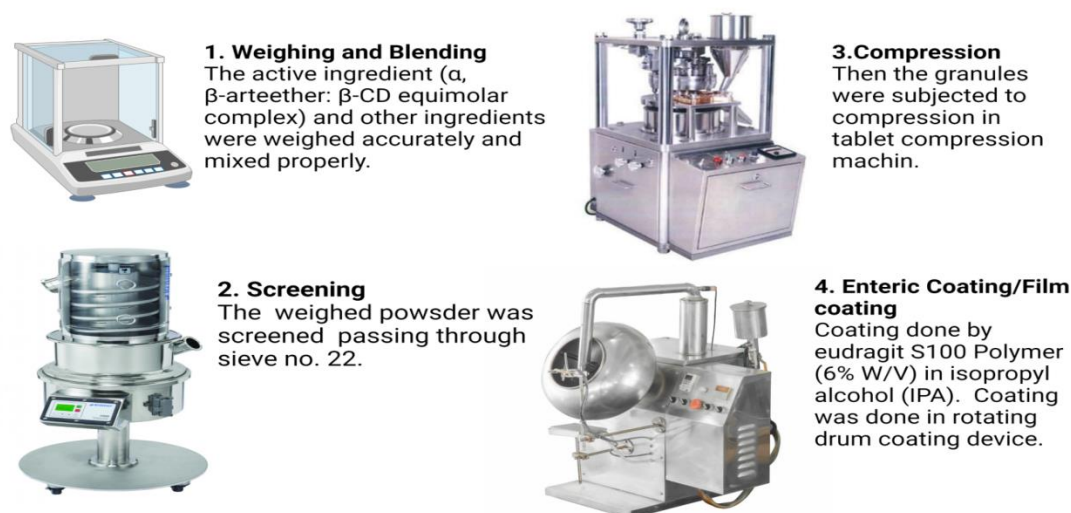


**Figure 4.10: The process of formulation development of enteric-coated tablets.**

#### **4.5.5.4 Formulation by design (FbD) strategy for optimization of critical variables of enteric coated tablets**

After identifying and analyzing potential risk factors, four excipients viz. diluent/binder excipient (microcrystalline cellulose), lubricant (magnesium stearate), and binder (PVP K30), Lactose as filler were selected as the independent variable for optimization and drug rest other factors were kept constant. A Box-Behnken design was employed for the optimization of enteric-coated tablets involving the least number of experimental runs. The low and high levels of factors selected for optimization were adopted after reviewing the literature and range mentioned in Pharmacopeia. The middle values were set as the midpoint of the low and high values of factors. % Drug release was selected as the response variable (dependent variable) for determining the optimized value of independent variables. Design Expert Version 13 (Stat-Ease Inc., Minneapolis, MN) was employed to investigate the relationship between the independent and dependent variables, developing a randomized design matrix and for statistical analysis. All the formulations involved were prepared in triplicate and evaluated. For determining the interaction between the two factors, one has to determine the effect of the first from the lowest level of the second factors, subtracting it from the value obtained after the effect of the first response at the highest level of the subsequent factors. The result of responses was obtained after the interaction of the selected independent variables and molded in the full second-order polynomial equation as shown in Equation 15

$$Y = \beta_0 + \beta_1X_1 + \beta_2X_2 + \beta_3X_3 + \beta_{11}X_1^2 + \beta_{22}X_2^2 + \beta_{33}X_3^2 + \beta_{12}X_1X_2 + \beta_{13}X_1X_3 + \beta_{23}X_2X_3 + \beta_{123}X_1X_2X_3 \dots \dots \dots (15)$$

where, Y is dependent variables or measured response,  $\beta_0$  is intercept,  $\beta_1$ ,  $\beta_2$  and  $\beta_3$  are linear coefficients,  $\beta_{11}$ ,  $\beta_{22}$  and  $\beta_{33}$  are the squared linear coefficients and  $X_1$ ,  $X_2$  and  $X_3$  are the studied independent variables.

#### **4.5.5.5 Defining of design space of enteric coated tablets**

According to ICH Q8 guidelines, design space is defined as “the multidimensional combination of the interaction of input variables (material attributes) and process parameters that have been demonstrated to assure quality”. Optimization in a combination of response surface methodology was employed for the design space establishment. In this case, Design space was established from a common operational range of selected CQAs viz. hardness and disintegration time. For finding the relationship between the independent variables and the dependent variables/responses, response surface methodology with help of Design Expert Software were employed for each of the parameters and any P value less than 0.05 was considered significant.

#### **4.5.5.6 Validation of model of enteric coated tablets**

For checking the accuracy and robustness of our model, the point prediction feature of Design Expert Software was employed. The point prediction feature in the software suggests the value of responses at a particular level of independent variables. The observed value of response after experimentation at the lab was compared to the predicted value of response for determining the % accuracy of the design model. Three batches were formulated using the optimized recipe for reducing the chance of error.

#### **4.5.5.7 In-process quality control (IPQC) evaluation of enteric coated tablets**

Employing Process Analytical Tools (PAT) throughout the process has granted wide importance in Food and Drug Administration (FDA) inclusive concept of QbD, involving efficient strategies for formulation design, process controls, and quality analysis, to attain the repetitive quantity of pharmaceutical products. Hence a plethora of in-process and finished product quality control tests were performed at various steps in the manufacturing of ODMTs to guarantee that manufactured product quality meets the expected profile. Various IPQC tests done during the formulation of ODMT with their possible effect on a quality profile were mentioned.



#### **4.5.5.7.1 Flow properties of enteric coated tablets premix powder**

Measurements of the bulk density, tapped density, Hausner's ratio, and Carr's index in triplicate using conventional techniques were used to examine the flow characteristics of premix powder.

The flow properties of tablet powder were determined as discussed in section (4.5.1.3.5) *Flow properties of SLNs*

#### **4.5.5.8 Finished Product Quality Control (FPQC) evaluation of enteric coated tablets**

Tests generally performed after the completion of the manufacturing process are known as finished product quality control tests. These tests are generally done for evaluating the qualitative and quantitative characteristics of the finished product and the acceptable range by which the manufactured item must comply during its shelf life. Various FPQCs done for quality evaluation of enteric-coated tablets are mentioned below:

##### **4.5.5.8.1 Weight variation test of enteric coated tablets (IP, 2007)**

To study weight variation, 20 tablets of each formulation were weighed using an electronic balance (CITIZON), and the test was performed according to the official method. Specifications for weight variation of tablets as per Indian Pharmacopoeia as given in Table 4.13.

**Table 4.13: Weight variation limits according to IP.**

<b>Average weight of tablet</b>	<b>Limit (% deviation)</b>
80 mg or less	10
More than 80 mg but less than 250 mg	7.5
250 mg or more	5

##### **4.5.5.8.2 Hardness of enteric coated tablets (USP, 1992)**

For each formulation, the hardness of 3 tablets was determined using the Monsanto hardness tester. The tablet was held along its oblong axis in between the two jaws of the tester. At this point, the reading should be zero kg/cm<sup>2</sup>. The constant force was applied by rotating the knob until the tablet fractured. The value at this point was noted in kg/cm<sup>2</sup>.

**4.5.5.8.3 Friability of enteric coated tablets (USP, 1992)**

For each formulation, the friability of 20 tablets was determined using the Roche friability. This test subjects a number of tablets to the combined effect of shock abrasion by utilizing a plastic chamber that revolves at a speed of 25 rpm, dropping the tablets to a distance of 6 inches in each revolution. A sample of pre-weighed 20 tablets was placed in Roche friabilator, which was then operated for 100 revolutions i.e. 4 minutes. The tablets were then dusted and reweighed. A loss of less than 1% in weight is generally considered acceptable. Percent friability (% F) was calculated as follows:

$$\%F = \frac{\text{Loss in Weight}}{\text{Initial Weight}} \times 100 \quad \dots\dots\dots(16)$$

**4.5.5.8.4 Content uniformity of enteric coated tablets (USP, 1992)**

CD complex containing enteric coated tablets were tested for their drug content uniformity. At random 20 tablets were weighed and powdered. The powder equivalent to a unit dose of tablet was weighed accurately and mixed in 100 mL of phosphate buffer (pH 6.8). The mixture was shaken properly. The undissolved matter was removed by filtration through Whatman No. 41 filter paper. Then the filtrate was subjected to acidic degradation with 5M HCl to induce chromophoric group to ART. The absorbance of the solution was measured at 254 nm. The concentration of the drug was computed from the standard curve of ART in phosphate buffer (pH 6.8).

**4.5.5.9 In vitro release studies of the enteric-coated tablets (USP, 1992)**

The ability of ART-CD enteric-coated tablet to remain intact in the physiological environment of the stomach was assayed by mimicking mouth-to-small intestine transit. The dissolution studies were carried out in 900 mL of 0.1N HCl for the first 2 h (as the average gastric transit time is (~ 2 h), then in a simulated intestinal fluid having pH 6.8 for the next 3 h (as average intestinal transit time) (Robinson & Lee, 1987). Drug release studies were carried out using the USP dissolution apparatus (Apparatus I, 100 rpm,  $37 \pm 0.5^{\circ}$  C). The height of the paddle was adjusted at about 2 cm above the bottom surface 10 mL of sample was withdrawn at regular time intervals.

Filtrates were then diluted with acetonitrile to release free drug comes into the organic phase due to high solubility in the organic phase, then the solution was subjected to

centrifuge so that all the other excipients were separated, then organic layer was separated and remove acetonitrile by evaporation, the solid residue after evaporation was subjected to acidic degradation with HCl and analyzed using UV Visible spectrophotometer (Perkin Elmer, Japan) at 254 nm for ART content. 10 mL of fresh medium was added to the dissolution vessel to make the volume after each sample withdrawal. *In vitro*, drug release studies of formulation were performed in triplicates.

#### **4.5.5.10 Permeability studies of prepared formulations**

On the intestine of a pig, permeability was measured in triplicate using the Franz diffusion cell procedure. The medium was phosphate buffer (6.8 pH). The benefactor chamber of the Franz cell was supplemented with an excess of ART and solid SMEDDs, lyophilized SLN, lyophilized NLCs, and cyclodextrin inclusion complex. The testing was performed by withdrawing 1 mL of the test and substituting the same amount of fresh media to ensure sink conditions at specific time points, (15, 30, 60, 90, 120, 240 and 360 min). The acquired sample was adequately diluted and introduced in the HPLC to examine the drug contained in the selection. After 6 h, the Franz diffusion cell was deconstructed, and the skin (from the diffusion research) was gently removed from the cell. The formulation was swabbed on the skin's surface with phosphate buffer. The treatment was done twice to guarantee no formulation residue remained on the skin's surface. After cutting the skin into tiny pieces, it was maintained in a buffer of pH 6.8 to extract the medication contained in the skin. After appropriate dilution and filtering, HPLC based method (section 4.3.9) was used to quantify the amount of drugs deposited in the skin.

#### **4.5.5.10 Ex-vivo studies of prepared formulations**

ART and ART-CD were screened against the chloroquine-sensitive (CQS, 3D7) and chloroquine-resistant (CQR, K1) strains of *P. falciparum*. Continuous *in-vitro* cultures of asexual erythrocyte stages of *P. falciparum* were maintained. Cultures were incubated at 37 °C in a gas mixture of 90 % N<sub>2</sub>, 5 % O<sub>2</sub>, and 5 % CO<sub>2</sub>. For IC<sub>50</sub> determinations, 20 µL of RPMI 1 640 with 5 µg/mL gentamicin were dispensed per well in an assay plate (384-well microtiter plate, clear-bottom, tissue treated). Next, 40 nL of each compound, previously serial diluted in a separate 384-well white polypropylene plate, were dispensed in the assay plate, and then 20 µL of a synchronized culture suspension (1 % rings, 10 % hematocrit) were added per well to

make a final hematocrit and parasitemia of 5 % and 1 %, respectively. The activity progress curves (fluorescence vs time) without and with inhibitors were analyzed by non-linear regression analysis (GraphPad software) using the pseudo-first-order equation. The antimalarial activity was done at CCMB, Hyderabad.

#### **4.5.5.12 *In- vivo studies of prepared formulations***

Male New Zealand rabbits weighing 2.5-3kg were procured from the Lala Lajpat Rai University of Veterinary, and Animal Sciences, Hisar, and housed in ventilated rabbit houses maintained at 24<sup>o</sup>C and 50% relative humidity. The animals were acclimated to the necessary temperature and moisture three days preceding the experiment. Before starting studies, the Institutional Animal Ethics Committee authorized the study procedures approved by IAEC (Approval number- MRSPTU/IAEC/2019/16). To determine and compare bioavailability ART aqueous suspension (ART dispersed in water), IV ART, IM ART, enteric-coated tablets, enteric-coated capsules filled with SLN, NLCs, spheroids and SMEDDS were administered separately. All the formulations were delivered orally at a 6 mg/kg dosage (except *i.m./i.v.*). The marginal ear vein was used for blood collection using microfuge tubes with spray-dried EDTA. After centrifuging the blood for 15 min at 2500 rpm, the plasma was collected, stored at 20<sup>o</sup>C temperature, and analyzed using HPLC.

##### **4.5.5.12.1 *Sample preparation***

Plasma was drawn from the rabbit's marginal ear vein and kept in EDTA-free tubes. The liquid was vortexed for 3 min after adding 0.4 mL acetonitrile and centrifuged at 25,000 rpm for 15 min at 10<sup>o</sup>C. The sample was followed by transferring the organic phase to fresh tubes, and auto sampler vials and injecting it into the HPLC for analysis.

##### **4.5.5.12.2 *Pharmacokinetics and biostatistics***

Pharmacokinetics and statistical analysis was also conducted to produce ART plasma concentration-time data. The maximal plasma concentration ( $C_{max}$ ) and the time required to attain that concentration ( $T_{max}$ ) were assessed using acquired data. The area under the concentration-time curve ( $AUC_{0-t}$ ) was analyzed using the trapezium technique. To determine  $C_{max}$  and  $T_{max}$ , individual animal concentrations were plotted against time. The absolute bioavailability of ART aqueous solution (ART dispersed in

water), IM ART, enteric-coated tablets, enteric-coated capsules filled with SLNs, NLCs, spheroids, SMEDDS, and enteric-coated tablets was calculated by dividing the respective AUC of each formulation by AUC of *i.v.* data. The value  $P < 0.01$  denoted statistical significance.